IMPACT OF STABILITY AND CONTROL ON VEHICLE GEOMETRY AND PERFORMANCE: A DESIGN STUDY ON TRADITIONAL HYPERSONIC VEHICLES VS CONTROL CONFIGURED VEHICLES

by

JUAN CAMILO BURITICÁ YATE

Presented to the Faculty of the Honors College of

The University of Texas at Arlington in Partial Fulfillment

of the Requirements

for the Degree of

HONORS BACHELOR OF SCIENCE IN AEROSPACE ENGINEERING

THE UNIVERSITY OF TEXAS AT ARLINGTON

May 2022

ACKNOWLEDGMENTS

I would like to acknowledge several people who accompanied me throughout this 4-year journey to become a professional aerospace and mechanical engineer. Without their help, this project, and the achievements I have collected throughout the semesters as the result of hard work would not have been possible without their influence and support.

First, I would like to extend my deepest gratitude and admiration to my senior design professor and mentor, Dr. Bernd Chudoba. His professionalism, vast experience, and knowledge of the industry and academia have helped me understand the application of the fundamentals of my career to the design of the most fascinating vehicles ever invented. His passion for teaching and his pursuit of knowledge has helped me become a better thinker, a better problem solver, and a student capable of receiving criticism as means of growth. For pushing my boundaries and allowing me to immerse myself in the vast world of aerospace engineering, I will be forever thankful. I would also like to thank my GTA, Cody Harris, for always being there to answer my doubts whenever I immersed myself in countless papers at the AVD lab. His knowledge and patience will always be appreciated.

Most importantly, I would like to thank my parents for all their efforts throughout the years to help me reach where I am today. For their discipline, unconditional love, support, and for always believing I could pursue higher standards of excellence, I will always be thankful. Finally, I would like to extend my gratitude to Emilia Cuervo. Her support and unconditional love helped me overcome the greatest challenges I encountered

throughout my college experience and constantly served as a role model I always strived to follow.

April 27, 2022

ABSTRACT

IMPACT OF STABILITY AND CONTROL ON VEHICLE GEOMETRY AND PERFORMANCE: A DESIGN STUDY ON TRADITIONAL HYPERSONIC VEHICLES VS CONTROL CONFIGURED VEHICLES

Juan Camilo Buriticá Yate, B.S. Aerospace Engineering

The University of Texas at Arlington, 2022

Faculty Mentor: Bernd Chudoba.

Hypersonic vehicles have been in development for over 60 years, yet a control-configure-vehicle has yet to be designed to understand the possible improvements over statically stable configurations. This paper studies the effect of stability and control on aircraft geometry and performance by comparing traditional vehicles versus control configured vehicles (CCV) that operate at subsonic and supersonic speeds and extrapolates this analysis to predict these effects on hypersonic vehicles. Data related to geometry, aerodynamic performance, and stability from various vehicles were collected and used to find trends by comparing aircraft design parameters to stability criteria. The results showed that by decreasing the degree of inherent static stability, the vehicles tend to become smaller and lighter but require more control power and advanced control systems to compensate. Based on these results, CCV design considerations applied to hypersonic vehicles as well as a Mach 5.2 Hypersonic Glider design point are discussed.

TABLE OF CONTENTS

LIST OF ILLUSTRATIONS

LIST OF TABLES

CHAPTER 1

INTRODUCTION

1.1 Extended Hypersonic Atmospheric Missions

The aerospace industry is moving at an accelerated pace towards breaking a new vehicle speed criterion: extended hypersonic flight. Hypersonic refers to speeds greater than five times the speed of sound (approximately 6,174 km/hr. or 3,836 mi/hr.). Flight at this speed has been achieved in the past and seen in space vehicles such as the Saturn V rocket designed by German aerospace engineer Werner von Braun, capable of not only taking the man to the moon but also accelerating its first stage to Mach 8 with its upper stages reaching even higher speeds. Another great example is the orbiter from the STS-Program, commonly known as the Space Shuttle, which is capable of reaching speeds during its ascent stage of Mach 22 and speeds up to Mach 25 during its re-entry. Three things these vehicles have in common are the high power provided by their respective rocket configurations (helped by the immediate availability of both fuel and oxidizer), reduced controllability (when compared to a fighter), and their well-optimized flight trajectories, which allow them to perform their mission while spending as less time in the lower atmosphere as possible. Based on these two examples, it can be shown that the modern problem with hypersonic flight is not necessarily reaching these speeds but performing extended missions through the lower earth atmosphere while also implementing design optimizations to achieve higher efficiencies and reduce operational costs.

Most of the relevant flight missions in the lower earth atmosphere can be commercial, such as transport of passengers and cargo, or military, such as interception, surveillance, and transportation of troops and cargo.

The next big jump in technology these fields are looking forward to is to obtain fleets that can travel at hypersonic speeds to make the world more accessible by reducing travel times significantly. These early steps towards high-speed atmospheric cruise were taken by military aircraft such as the SR-71, capable of cruising and maneuvering at speeds of Mach 3+ during its surveillance missions, or the Concorde, which reduced the trans-Atlantic travel from Paris to New York from 8 hours to around 3.5 hours. The latter vehicle had one of the most advanced designs and state-of-the-art technology for commercial aviation. Still, its business model, mainly affected by government regulations pertaining to sound pollution and sonic boom over land, proved to be unsustainable, eventually leading to its retirement in 2003. Concorde is a great example that leaps in technology do not assure that new things will remain sustainable for future generations. In the case of high-speed flight, the engineering/technical aspect is not the only area of importance for the success of aircraft development.

The main obstacles producing technical limitations for the hypersonic cruise are the physical conditions that arise when traveling at those speeds, which severely compromise the current aircraft technologies. Vehicles traveling at hypersonic speeds cause the air to compress excessively, leading to extreme thermodynamic and chemical conditions that cause the air to reach high temperatures, which can compromise the structure of aircraft if built with common materials such as aluminum or modern composites. Moreover, thermal resistant materials such as titanium tend to be more expensive and heavier in most cases, so the vehicle's shape must be aerodynamically optimized to minimize the required exposure of the airframe to such critical conditions in an effort to save weight and funds in materials. Unfortunately, the designs that are optimized with a focus on the hypersonic portion of the mission tend to have poor lift to drag ratios, especially at subsonic speeds; hence poor performance and powerful propulsion systems are required to accelerate these vehicles properly. These are just a few of the technical aspects that are challenging to properly engineer, and definitive connections and dependency amongst the various engineering disciplines can be seen, making the design of hypersonic vehicles a multidisciplinary task that requires advanced design methods such as Hypersonic Convergence that allow to properly size the vehicle with a more holistic approach considering the requirements of various disciplines from the early stages of conceptual design.

Hypersonic sustained flight not only requires developing state of the art technology to push the physical frontiers even further but also learning from the mistakes of its predecessors; although they are not flying today, their research, developments, and experience are the rich foundation upon which the new era of flight is being built. As presented by the previous lines and the imminent relevancy of this future technology, it is the duty of the new generation of aerospace engineers to put focus on this technology which could bring us closer together or take us apart were it be used for the wrong purposes, to understand and manipulate its potential fully. The work of this project will support this endeavor by providing a disciplinary insight focused on stability and control of hypersonic vehicles to understand how its realization in different configurations, traditional versus control configured, affect the performance and the overall geometry.

1.1.1 Background on Hypersonic Vehicles

Hypersonic vehicles can travel at speeds greater than 5 times the speed of sound. Developing such aircraft is one of the greatest feats of the aerospace industry, considering the rapid evolution that took place in a 40-to-50-year window between the first flight of the Wright brothers at Kitty Hawk to the powerful rockets designed by Dr. Werner Von Braun and the challenging aerospace vehicles designed by Dr. Eugen Sänger both during the second world war. The technology to make these vehicles possible has been in development for over 60 years, reaching fields from aerodynamics and material science to high-speed propulsion. Designing such type of aircraft is, of course, complicated, mainly due to the high level of integration of the various technologies corresponding to each discipline. For a design to be successful, it needs to converge at a design point that satisfies the requirements of each field to a certain degree.

The aerodynamics of hypersonic vehicles is complex mainly due to the extreme thermodynamic conditions that arise at such high speeds. The aerospace industry was accustomed to the theories that could ideally describe the behavior of incompressible fluids such as the ones postulated by Ludwig Prandtl and compressible flows through high subsonic-supersonic theories such as the ones postulated by Theodore Von Kármán. These theories would allow aerospace engineers to determine the aerodynamic performance of a configuration for the speed needs of the time, where vehicles could not exceed the region of low supersonic. As described by Weiland [1], at hypersonic speeds, vehicles do not only deal with compressibility effects at high speeds but also harsh aerodynamic phenomena that cause gases around the vehicle to lose their ideal gas behavior commonly employed for conventional thermodynamic calculations, turning into a mix of dissociated nitrogen and oxygen molecules as well as plasma. These effects change the pressure, and the shear stress fields of the flow, slightly affecting the pressure distribution linked to pressure drag but having a more notorious effect on the skin friction drag due to alterations to the air's viscosity at high temperatures. This has made the aerodynamics of hypersonic vehicles heavily dependent on the study of unsteady heat transfer, giving rise to the aerothermal discipline, which focuses on studying the thermodynamics of the air-airframe interactions and allows engineers to understand which parts of the vehicle are critical in terms of extreme temperatures experienced at hypersonic speeds which of course have a detrimental effect to the structure of the aircraft [1].

Moreover, due to the increase in skin friction and wave drag, hypersonic vehicles tend to have poorer L/D values, which for the SAENGER II, one of the most studied and optimized designs, had a max L/D of around 9 at Mach 0.5 and barely exceeded and L/D of 4 at Mach 7[1]. This leads to another technical issue, which is the selection of the wing and airframe shapes that could offer better performance at hypersonic speeds. One solution to this is the hypersonic waverider concept developed, where the vehicle has an optimized leading edge that allows the shockwave formed at the cruise Mach number to be formed along the leading edge, perfectly sealing and avoiding the higher pressure of the underbody to leak into the upper body suction, hence reducing effects such as induced drag and the maintaining the high pressure in the underbody, hence more generating more lift, which results in the best L/D ratio achieved by a hypersonic body shape that is not an infinitely thin plate [2]. Unfortunately, this improved L/D geometry comes at a penalty of reduced internal volume, making it difficult to use for missions requiring a significant payload for cruise or orbital missions. Alternatives to the waverider, that although they do not offer the same aerodynamic performance, offer better payload capabilities are the blended wing body such as the SAENGER II or the lifting body used by the X-30 National Aerospace Plane Program. Using a blend of this geometries may allow to converge to a useful configuration, but to compensate for losses in aerodynamic performance, powerful propulsive technologies are required.

In terms of propulsion, hypersonic vehicle concepts tend to make use of airbreathing technologies, that is, engines capable of using the oxygen of the immediate atmosphere to achieve proper combustion. These types of engines remove the requirement of having to carry an oxidizer tank in addition to the fuel required to complete the mission, which produces critical volumetric and weight savings that improve the overall performance of the vehicle. One such technology is turbine combined cycles (TBCC), which make use of a specific type of engine for a given speed, providing high performance throughout the flight envelope. These configurations tend to include a first engine stage that can either be a turbojet or a turbofan which can successfully operate from take-off to speeds of up to Mach 3. When the vehicle reaches Mach 3, the levels of compression cause the temperature to increase and generate supersonic conditions at the tip of the turbine blades, which could compromise the engine's structure and a decrease in ISP. When this happens, a Ramjet stage can be included in the engine configuration to take advantage of the compression taking place at high Mach numbers by incorporating a variable geometry duct that compresses the air by generating a series of shocks that progressively decrease the airspeeds of the mass flowrate coming into the engine with better efficiency. Aircraft that have used this Turbojet-Ramjet combined cycle was the SR-71 which used 2 Pratt and Whitney J-58 engines, each with a Ramjet coaxially installed, which made use of the variable geometry allowed by the world-famous moving spike. For vehicles requiring more thrust at high supersonic or hypersonic speeds (greater than Mach 6), the inclusion of scramjets can be theoretically evaluated due to their better ISP at these speeds. Scramjets, or Supersonic Combustion Ramjets, operate in a similar fashion to Ramjets. Still, as the name suggests, the difference lies in the combustion speed, which for scramjets is supersonic instead of the subsonic requirement for ramjets. This type of engine is a state-of-the-art technology that is still being tested to produce thrust at a significant scale so that it can be employed for bigger vehicles than the X-51. From a geometry standpoint, the TBCC must be properly integrated into the already complex airframe in such a way that it can capture the required mass flow for normal operation at good efficiency. For this, different types of inlets such as compression ramps (which make use of the forebody compression) and geometries derived from supersonic flow fields such as the Busemann inlet have been developed to make such integration possible.

As can be seen, making a successful hypersonic configuration is not an easy task because every discipline has specific requirements and ideal design specifications, which oftentimes get truncated by other disciplines. Because of this, hypersonic vehicle design is a multidisciplinary effort where proper sizing tools and a well-structured team dynamic where each member understands the basic flow of Input-Analysis-Output of the disciplines involved becomes a requirement to develop a successful configuration.

1.1.2 History of Aircraft Control Systems

The control of aircraft has been a key component of design since the invention of the first working heavier-than-air aircraft by the Wright Brothers in 1903. In the first model, the brothers knew that to properly maneuver the aircraft, control surfaces needed to be added to produce the necessary pitching, yawing, and rolling moments during flight. The first approach to add maneuverability was adding three sets of controls that the pilot could use to induce the required moments. The first control was a lever that controlled the control effectors located in the canard of the aircraft, allowing changes in lift that produced pitching moments in the Y axis. The second control was a lever that deflected the rudder located behind the vehicle to produce lift in the Y axis of the vehicle producing the yawing moment in the Z axis. The third control, and certainly cleverer, was using the pilot's weight to warp the wing. The pilot was suspended in a harness that was connected to a set of cables that, when tensed or compressed (depending on the side the pilot is shifting towards), would produce changes in the angle of attack of the tips of the wing, which would induce rolling moments about the X axis of the vehicle due to changes in the lift produced by either side of the wing [3]. One aspect that the brothers did not consider was the influence of stability on the controllability of the aircraft; in the Canard-Wing configuration, the Wright brothers produced a neutral point located at 10% of the cord from the wing's leading edge and had a center of gravity location of 30% of the cord from the same datum which generated a static margin of -20% which produced unstable nose up pitching moments. This negative static margin is very high compared to aircraft that use automatic control for which the greatest negative static margin allowed is 5% [4]. This made the vehicle hard to control by requiring constant inputs from the pilot to correct attitudes and maneuver the vehicle, which increased the pilot's fatigue causing multiple crashes. During the World War II era, the demand for bigger vehicles increased to transport bigger payloads. To achieve this, the inclusion of powerful hydromechanical systems played a key role in making aircraft bigger by deflecting bigger surfaces as well as resisting stronger hinge moments. Although powerful, hydromechanical systems also had some flaws, such as the high pressure at which they operated, which in case of a failure, could burst in the middle of the flight, and also its weight. As decades passed, the hydromechanical systems were upgraded, adding features such as irreversible controls, which avoided the pilots from dealing with great forces. Moving into more recent times, the advanced hydromechanical systems were soon outdated with the development of the Fly-by-Wire during the 1970s. Fly-by-Wire replaces the manual control mechanisms such as pulleys, rods, linkages, etc., for computers, wires, and electrically controlled hydraulic actuators, which not only allowed to save weight but also fine-tune the desired handling qualities of the vehicle even more. This technology has become the normal level of technology in modern-day airliners and other types of aircraft due to their high levels of redundancy, which tend to be safer, and the increased control performance compared to more bulky and old systems. Technology has not changed much since the implementation of such a system, but similar implementations such as Fly-by-Light have promised better response times and more weight reductions. When it comes to cutting-edge technology, Plasma actuators or Active Flow Control could become a game-changer if their design can provide enough control power to compete with older and more reliable systems. This system accelerates the flow over a surface without having any mechanism to produce a deflection. It achieves this by creating a difference in potential across two electrodes, generating a plasma discharge that accelerates the air on a given surface, changing the pressure distribution, and producing the required forces (ideally) [3].

1.1.2.1 Stability and Control Augmentation Systems

Aircraft behavior can be mathematically modeled as a dynamic system whose characteristics can be evaluated and altered as needed to produce satisfactory time responses, commonly known as handling qualities. Determining optimal handling qualities is a joint effort that requires inputs from both engineers and pilots to arrive at a configuration whose characteristics can be evaluated numerically (via damping ratios and time constants of the multiple dynamic modes, system stability, etc.) as well as the pilot's feel. Stability augmentation systems (SAS) were initially developed to improve the damping characteristics of the vehicle. This system consists of a feedback loop that sensors an aircraft motion parameter and produces an additional control effector deflection to counteract the motion, enhancing the damping [5]. This is performed automatically without input from the pilot, whose delayed response time is not suited for this kind of correction. During the 1950s, on aircraft such as the F-4 and the F-104, this system was embedded into the hydromechanical system required to transmit the pilot's input to the different control effectors, and the control authority (percentage of total surface deflection available) was limited to 10%. This system had the main problem: due to the feedback loop, it also ended up opposing the pilot's input, decreasing the vehicle's responsiveness [5].

As technology progressed, Control Augmentation Systems (CAS) improved upon SAS's issues by sending the pilot's input signal through both the mechanical system and the onboard computer. This removed the feedback loop issue opposing the pilot's input and allowed for the control authority to be increased to 50% [5].

Shifting to modern times, most aircraft use Fly-by-Wire systems, which make use of control augmentation. Still, instead of using heavy mechanical systems, the communication is replaced via electrical signals that are sent by the flight computer to actuate the different control effectors of the aircraft. This modern system makes use of triple or quad-redundancy to increase its reliability, and its full authority allows for fine-tuning the stability and control characteristics of a given vehicle depending on the mission[5].

1.2 Longitudinal Static Stability

Longitudinal Static Stability refers to the tendency of an aircraft configuration to return to its original attitude after a perturbation by virtue of the aerodynamics forces and moments produced by the airframe without any control effector input. This parameter which is represented by the aerodynamic derivative C_{m_α} relies heavily on a factor called the static margin. The static margin is the distance between the vehicle's center of gravity and its neutral point. The neutral point is that location along the longitudinal axis, after which the center of gravity cannot travel without making the configuration unstable in pitch. In positive static stability, the center of gravity lies ahead of the neutral point; hence when the vehicle is perturbed, it will return to its original attitude without any input. For Relaxed static stability, the center of gravity lies very close to the neutral point (or even exactly at that location); hence after a perturbation, the vehicle will remain in the new attitude unless external forces are applied. For Negative Static Stability (unstable), the center of gravity lies behind the neutral point. After a perturbation, the vehicle will tend to oscillate about the original attitude. The amplitude of such oscillation will increase with time, which can produce loss of control if not taken care of. This type of stability is estimated by referring to the sum of moments of the aircraft about the center of gravity and adding the contribution of each component of the configuration. This equation is then normalized to deal in terms of the moment coefficient equation. One thing to note is that for the pitching moment equation, there is a significant dependence on the angle of attack at which the moment is evaluated. By differentiating the pitching moment coefficient equation with respect to the angle of attack and setting it equal to 0, one may solve for the neutral point at a given flight condition. The neutral point for tail aft configuration is far more involved due to the number of components as well as the complexity of their estimation. For tailless aircraft, however, the derivation of moments and the derivative with respect to the angle of attack is straightforward if one assumes the vehicle to behave like a flying wing which results in a neutral point located at the aerodynamic center of the vehicle, which is the case for most hypersonic vehicles. For a stable configuration, the stability derivative should be negative, as shown in Eq. (1)

$$C_{m_\alpha} < 0 \tag{1}$$

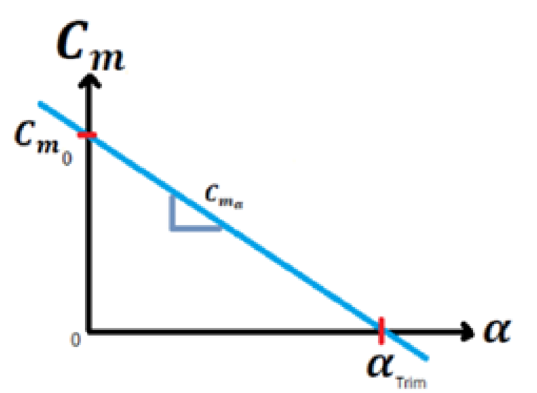

Figure 1.1: Moment Coefficient Curve of a Stable Aircraft

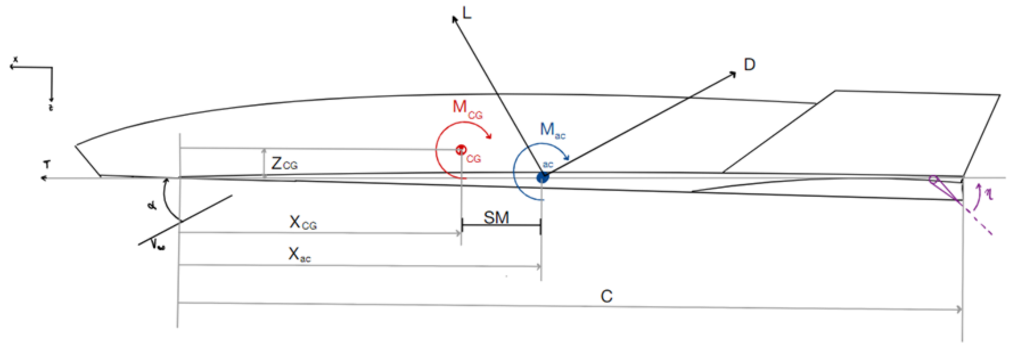

Figure 1.2: Reduced Order Model of a Hypersonic Vehicle

1.3 Influence of Stability and Control on Performance

The performance of an aircraft is evaluated based on the mission requirements set before the conceptual development takes place. The most relevant performance criteria are the range, endurance, rate of climb, and maneuverability (which is dictated by the g's the vehicle can produce and support without compromising its structure). One key aspect that unites these criteria is their dependence on aerodynamic performance, where the lift and drag play a key role in the vehicle's performance. The set of Breguet equations, one of the most important and well-known in aeronautics, provides a good reference for the range and endurance of a vehicle while cruising at a steady-state and constant specific impulse. As shown by equations (2) through (5), for these sets of basic flight conditions, the maximum distance the aircraft can travel as well as the time it can loiter is directly proportional to the L/D ratio. Furthermore, the rate of climb, which is the vertical speed of the vehicle has as it climbs and from which time to cruise altitude can be obtained, shown in, also shows a dependency on drag which in order to be maximized, the drag encountered should be less than the thrust produced, which leads to max L/D if minimum drag is used. These set of equations are meant to be used at different points of the trajectory due to the variation of aerodynamic and fuel consumption conditions encountered during normal operation

- Breguet Range and Endurance equations for Constant Speed/Constant C_L [6]

$$\boldsymbol{R = \frac{V}{c}\left(\frac{L}{D}\right)\ln\left(\frac{w_i}{w_f}\right)} \tag{2}$$

$$\boldsymbol{E = \frac{1}{c} * \left(\frac{L}{D}\right)\ln\left(\frac{w_i}{w_f}\right)} \tag{3}$$

- Breguet Range and Endurance equations for Constant altitude/ Constant C_L [6]

$$\boldsymbol{R = \frac{1}{c}\left(\frac{2\sqrt{2}}{\sqrt{\rho S}}\right)\left(\frac{\sqrt{C_L}}{C_D}\right)\left(\sqrt{w_0} - \sqrt{w_i}\right)} \tag{4}$$

$$\boldsymbol{E = \frac{1}{c} * \left(\frac{L}{D}\right)\ln\left(\frac{w_i}{w_f}\right)} \tag{5}$$

- Rate of Climb [7]

$$\boldsymbol{ROC = \frac{T - D}{W} * V} \tag{6}$$

Stability and control come into play in the minimization of drag to maximize the L/D and hence improve the performance characteristics shown by the equations above. The main way this can be done is by making the aircraft less stable. As discussed in the previous subsection, a certain degree of static stability is desired depending on the mission. This stability acts as a support for the pilot and has an impact on trim drag. When an aircraft wants to reach steady-state conditions, it wants to do so by balancing the forces and the aerodynamic moments. Since the aircraft has an inherent pitching moment due to the geometry of the configuration, additional help from the control effectors is needed to produce the required moments to bring the sum of moments to zero and hence achieve trim. This is performed by deflecting such control effectors to produce the necessary vertical force to cause the aircraft to rotate. Still, this increase in lift (regardless of direction) increases the induced drag at the control effectors, which adds to the overall drag of the vehicle, decreasing the total L/D, and having a detrimental effect on the performance. This effect varies depending on how inherently stable the vehicle is—the more stable, the more force needed to overcome the restoring moments, the more induced drag.

1.4 Influence of Stability and Control on Aircraft Geometry

Most of the efforts to involve stability and control in the optimization and improvement of aircraft performance have been achieved by implementing either RSS or unstable static stability in addition to an onboard active control system to compensate. Studies such as the one performed by Sliwa [8] on commercial aircraft design, as well as the studies performed by Walker [9] on developing controlled configured tankers, showed great results in control effector surface area reduction, mainly in the horizontal tail (where the area was significantly reduced or even entirely removed) as well as the surface of the wings. These reductions not only helped the configurations reduce their overall drag attaining greater L/D values but also decreased their weight which improved their T/W. In addition to this, a comprehensive study performed by Hepler et al. [10] determined that the control configured version of the re-entry vehicles tended to have reductions in control surfaces as well as fixed wing area. This study also showed how dominant the tanks become for hypersonic vehicles by quoting the authors *"This results in the vehicle configuration* *being shaped by the tanks.”*. Walker et al. also provide an interesting fuel tank placement trade study of tank allocation, where they concluded that placing the LOX tank aft rather than forward produced weight and volume savings due to changes in the shape of the tanks. This inclusion of LOX would be out of bounds for TBCC configurations, but a similar study for dual fuel configurations could be performed to assess their viability over single fuel configurations.

1.5 XB-70 Case Study

The XB-70 Valkyrie was a supersonic bomber capable of reaching speeds of Mach 3 developed during the 1960s. This vehicle is well known for its ability to fold its wing tips downwards whenever it is cruising at supersonic speeds. The influence of stability and control in performance provides insight into this design decision. When the aircraft enters the supersonic regime, its aerodynamic center shifts aft by a significant margin, and in the case of this vehicle, the shift was from around 27% to near 40% of the chord. In a study presented by Wolowicz et al. [11], it can be seen that the center of gravity location remains relatively constant throughout the trajectory around 19-22% of the chord. Having a fixed center of gravity and an aerodynamic center/neutral point shifting aft as speed increases progressively increases the static margin making the vehicle overly table. As explained in the performance section, having a vehicle with a high stability margin causes a lot of trim drag due to the need to generate higher forces to trim the aircraft. It is at this point that the wing tips come into play. For a regular delta wing, the lift distribution tends to be greater towards the base of the triangle due to the sweptback nature of the platform, causing the aerodynamic center to lie more towards the rear of the vehicle. When the XB-70 drops its wingtips, it destroys the lift distribution towards the rear of the vehicle, causing the aerodynamic center to shift forward, as can be seen in Figure 1.3. This forward shift of the aerodynamic center reduces the static margin making the vehicle more maneuverable while also requiring less control effector force to change attitude and trim, hence improving the performance of the XB-70. A technical summary of the configuration changes is presented in the Reduced Order Model shown in.

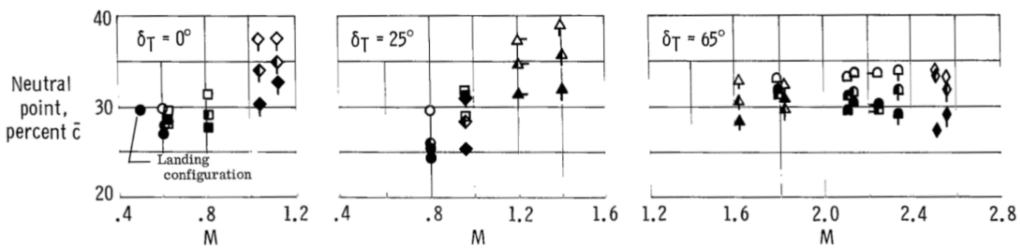

Figure 1.3: XB-70 Neutral Point Location vs. Mach Number [11]

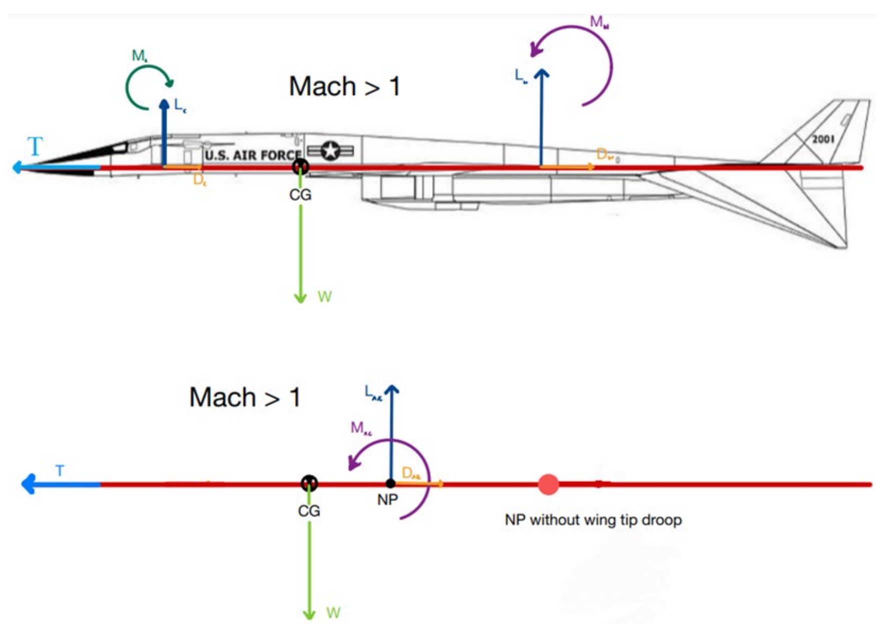

Figure 1.4: Reduced Order Model of the XB-70 [13]

CHAPTER 2

LITERATURE REVIEW

2.1 Main References

For this study, a literature review on the characteristic of controlled-configured-vehicles was reviewed to obtain adequate definitions as well as the necessary aircraft data to identify the possible design tradeoffs when comparing such vehicles against the more traditional configuration. One of the main findings is that there are two main categories for CCV design. The first of them, and most important for the purposes of this project, is the development of vehicles with relaxed or unstable static stability from the conceptual design. The references that possessed this kind of approach often provided a baseline configuration that was significantly more stable and provided the necessary data to show how the geometry and aerodynamic performance gains evolved as the configurations became less stable. The second category for controlled-configured-vehicles is the vehicles designed with inherent stability in mind. Still, a CCV variation is produced utilizing the same airframe but re-arranging the weight distribution to reduce static stability while improving the augmented control system to further fine-tune the design. These vehicles are useful when studying the effects of the reduced static margin but do not show the effects on aircraft geometry through the conceptual design stage, which is the main purpose of this study. Table. 2.1 summarizes the academic sources reviewed for this study.

Table. 2.1: Literature Review

Title	Author	Summary	Ref
Stability and Control of Conventional and Unconventional Aerospace Vehicle Configurations	B. Chudoba	The author presents a methodology to assess stability and control on aircraft from the early stages of conceptual design by developing and implementing his tool Aeromech	[14]
An MDO approach to Control-Configured-Vehicle design	M.R. Anderson W.H. Mason	Presents a multidisciplinary optimization methodology for CCV in conceptual design by evaluating different levels of flight control system complexity	[15]
Applicability of the Controlled Configured Design Approach to Advanced Earth Orbital Transportation Systems	A. Hepler H. Zeck	Comprehensive study on the effects of unstable re-entry vehicle configurations similar to the space shuttle where they evaluate multiple effects on weight distribution, surface sizes, dynamic responses, and surface deflections required for hypersonic trim at high angles of attack	[10]
Tailless Aircraft Performance Improvements with Relaxed Static Stability	I. Ashkenas D. Klyde	The authors present the effects of RSS on the YB-49 flying wing configuration	[16]
Air Superiority with Controlled Configured Vehicles	J. Krachmalnick S. Lafavor	Study of RSS on the F-4 Phantom, where improvements in maneuverability and drag reduction were obtained. Variation of different performance parameters versus the c.g. location is presented.	[17]
Design of a Control Configured Tanker Aircraft	S. Walker	Study on geometry and weight changes and performance improvements of a baseline tanker configuration vs. control configured configuration.	[9]
Impact of Longitudinal Flying Qualities Upon Design of a Transport with Active Controls	S. Sliwa	Author presents a detailed study of a CCV commercial aircraft design, showing the results of multiple iterations while changing the SM from 20% to 10%. The study presents	[8]

		geometry reductions and L/D improvements	
The CCV Fighter Program	F. Swortzel A. Barfield	The study presents the results of CCV modifications to an existing version of the F-16 fighter by including an enhanced Fly-by-Wire system as well as a new vertical canard configuration	[18]
Elevator Sizing, Placement, and Control-Relevant Tradeoffs for Hypersonic Vehicles	J. Dickeson A. Rodriguez S. Sridharan	Authors present a non-linear model capable of showing the influence of control size and allocation of a hypersonic scramjet-powered vehicle on the aerodynamics and dynamics of the system	[19]
Static Stability and Control of Hypersonic Gliders	R. Rainey	Study on the static stability of hypersonic boost glide where required airframe geometries and control deflection for trim at an angle of attack range of 6-45 degrees were explored	[20]
Stability and Control in Aircraft Design	J. Wimpenny	Author presents information on optimized wing shapes to cross the sound barrier	[21]
Control Allocation Challenges and Requirements for the Blended Wing Body	D. Cameron N. Princeton	Authors provided information on the effect of surface size on the deflection rates, hinge moments, and actuator power requirements	[22]
Airplane Design Part VII: Determination of Stability, Control, and Performance Characteristics	J. Roskam	Mathematical models to estimate performance parameters as well as information on how to improve L/D by changing the wing design.	[7]
Introduction to Aircraft Flight Mechanics	T. Yechout	General information on Static Stability and Types of Control Systems	[5]
Untersuchung der Separationsdynamik eines zweistufigen Hyperschall-Flugsystems unter besonderer Berucksichtigung der Seitenbewegung	C. Zahringer	Geometry and Aerodynamic Data for the SAENGER II	[23]
Selected Aerothermodynamic Design Problems of Hypersonic Flight Vehicles	C. Weiland	Information about control volumes and characteristics of SAENGER II	[24]
Aerodynamic Data of Space Vehicles	C. Weiland	Aerodynamic information of SAENGER II	[1]
The Longitudinal Static Stability of Tailless Aircraft	H.V. de Castro	Presents a methodology to estimate the moment coefficient	[25]

		derivative with respect to the angle of attack for tailless configurations	
Trajectory and Flight Mechanics Analysis of the HEXAFLY-INT Experimental Flight Vehicle	Morani	SM margin along the trajectory at Mach 7 of the HEXAFLY-INT vehicle	[26]
The Evolution of Flight Control Systems	H. Al Hami A. Aslam	Authors present a complete evolution of flight control technologies from the wright flyer to modern aircraft	[3]
The Aerodynamic Design of Aircraft	D. Kuchemann	Author presents a comprehensive analysis of aerodynamic design as well as geometry relations applicable for waveriders	[27]
Aerodynamic Characteristics and Control Effectiveness of the HL-20 Lifting Body Configuration at Mach 10 in Air	W. Scallion	Study on control effectiveness of a Mach 10 Lifting Body	[28]

In addition to the literature review, multiple online sources were consulted to obtain the required aircraft design data to perform the analysis of this project. Table. 2.2 contains a summary of the reviewed vehicles as well as the references from which data was obtained.

Table. 2.2: Aircraft References

Aircraft	Type	Year	References
ASCAC	CCV	1980	[15]
YF-16	CCV	1978	[18,29]
F-4 Phantom	CCV	1958	[30]
Tanker (CCV)	CCV	1973	[9]
F-117	CCV	1981	[31–33]
B-2	CCV	1989	[34]
X-29	CCV	1984	[35,36]
Sliwa V2	CCV	1980	[8]
Sliwa V3	CCV	1980	[8]
YB-49	CCV	1947	[37]
HEXAFLY-INT -PAX	CCV	2017	[26]
SAENGER II	CCV	1980	[1,23,24]
Tanker (CON)	Traditional	1973	[9]
Concorde	Traditional	1969	[38]
Sliwa V1	Traditional	1980	[8]
XB-70	Traditional	1964	[11]
Learjet 36A	Traditional	1973	[39,40]
Boeing 747-400	Traditional	1969	[41–43]

CHAPTER 3

METHODOLOGY

This chapter will focus on explaining the methodology for the project. This project presents a design study for estimating the geometry of a control-configured-vehicle that, by virtue of its relaxed or unstable static stability, is capable of providing improvements in aerodynamic performance (which directly influences the overall performance as shown by the previous sections) as well as weight savings.

The first step of this method was choosing the adequate CCV approach for this project. As described in the previous sections, some of the literature considers CCVs as those vehicles that have had stability and control optimization from their inception, while other sources also include those vehicles whose airframe already existed but got improvements in the control system and weight distribution to achieve RSS (such as the YF-16 and the B-52 CCV variation). Since the senior capstone course is focused on the conceptual design from a multidisciplinary approach, the first definition was chosen to build the methodology. Once the concept of CCV was defined, it was decided that a classical approach for integrating stability and control characteristics by estimating CE dimensions and desired static margin from trends of previous vehicles. For this, a database containing both CCV and traditional aircraft had to be built to obtain the most common geometric relations for CCVs and compare the configuration changes when we analyze vehicles with inherent static stability to those with RSS or unstable configurations. Since this project's scope is focused on the hypersonic regime, multiple sources of real vehicles were consulted as an initial step. Unfortunately, most of the vehicles studied were scaled models with no information on how the full-scale vehicle would behave.

For this reason, the SAENGER II and the HEXAFLY-INT (continuation of the LAPCAT project) vehicles were the only hypersonic vehicles included in this database. Due to the small number of hypersonic vehicles, it was decided to produce a comparison between CCVs and traditional subsonic and supersonic vehicles and then extrapolate their trends to the hypersonic regime. For this, it was decided to categorize as CCV those vehicles with RSS or negative static margins and as Traditional those vehicles with positive static margins. Please refer to Table. 2 for the selection of vehicles in this study. In the same way that sizing a vehicle is not a matter of simply photographically scaling its features and assuming it will work in other conditions, it is also important to note that after the trends have been identified, they will be evaluated with criteria from other disciplines to provide an educated conclusion of their feasibility in the hypersonic environment.

Once the vehicles were selected, the design characteristics are summarized in Table. 3 were obtained to populate the database. Most base information about the vehicles was obtained from academic sources or online sites, but some parameters had to be estimated. Data Image Correlation method using MS paint was used to measure distances and surfaces that were not given for any of the vehicles. This process consists of obtaining an accurate 3-view of the vehicle and then determining a Pixel/ft scale that we can use to measure distances in the image and then scale back to real dimensions. The author presents the verification of such a method [44]. For this project, the volume coefficient of the control effectors was estimated using the reference dimensions used by Weiland [24] to make the process more general for all vehicles. The complete database can be found in Appendix B, and the DIC estimations can be found in Appendix C. A summary of the methodology is presented in the NS Diagram in 3.1.

Table. 3.1: Data Base Parameters

Parameter	Symbol	Estimation
CRUISE MACH	M	AC Data
Take-off Gross Weight	TOGW	AC Data
Operating Weight Empty	OWE (lbs.)	AC Data
Thrust	T (lb.)	AC Data
Planform Area	S_wing (ft^2)	AC Data
Wing Loading	W/S (psf)	AC Data
Thrust to Weight Ratio	T/W	AC Data
Aspect Ratio	AR	$AR = \frac{b^2}{S}$
Span	b (ft)	AC Data
Mean Aerodynamic Chord	MAC (ft)	AC Data or $MAC = \frac{2}{3} c_r \left(\frac{\lambda^2+\lambda+1}{\lambda+1}\right)$
Full Length	L_f	AC Data
Vertical Tail Area	S_V (ft2)	AC Data Or DIC
Horizontal Tail/Elevon Area	S_{HO} (ft2)	AC Data Or DIC
center of gravity location (% of Lf)	X_{cg}/c	AC Data
Static margin	SM	$SM = \frac{(X_{np} - X_{cg})}{MAC}$
Maximum Lift-to-Drag ratio	$(L/D)_{MAX}$	AC Data
Slenderness Ratio	f_r	$S_r = \frac{0.5b}{L_f}$
Longitudinal CE Moment Arm	L_{LoCE}	$L_{LoCE} = X_{ac-LoCE} - X_{cg}$ and DIC
Directional CE Moment Arm	L_{DiCE}	$L_{DiCE} = X_{ac-DiCE} - X_{cg}$ and DIC
LoCE Volume Reference	V_{LoCE} REF	$V_{LoCE-REF} = S_{pl} * L_f$
DiCE Volume Reference	V_{DiCE} REF	$V_{DiCE-REF} = S_{pl} * b$
LoCE Volume Coefficient	$\bar{V}_{LoCE}$	$\bar{V}_{LoCE} = \frac{S_{HO} * L_{LoCE}}{V_{LoCE-REF}}$
DiCE Volume Coefficient	$\bar{V}_{DiCE}$	$\bar{V}_{DiCE} = \frac{S_V * L_{DiCE}}{V_{LoCE-REF}}$

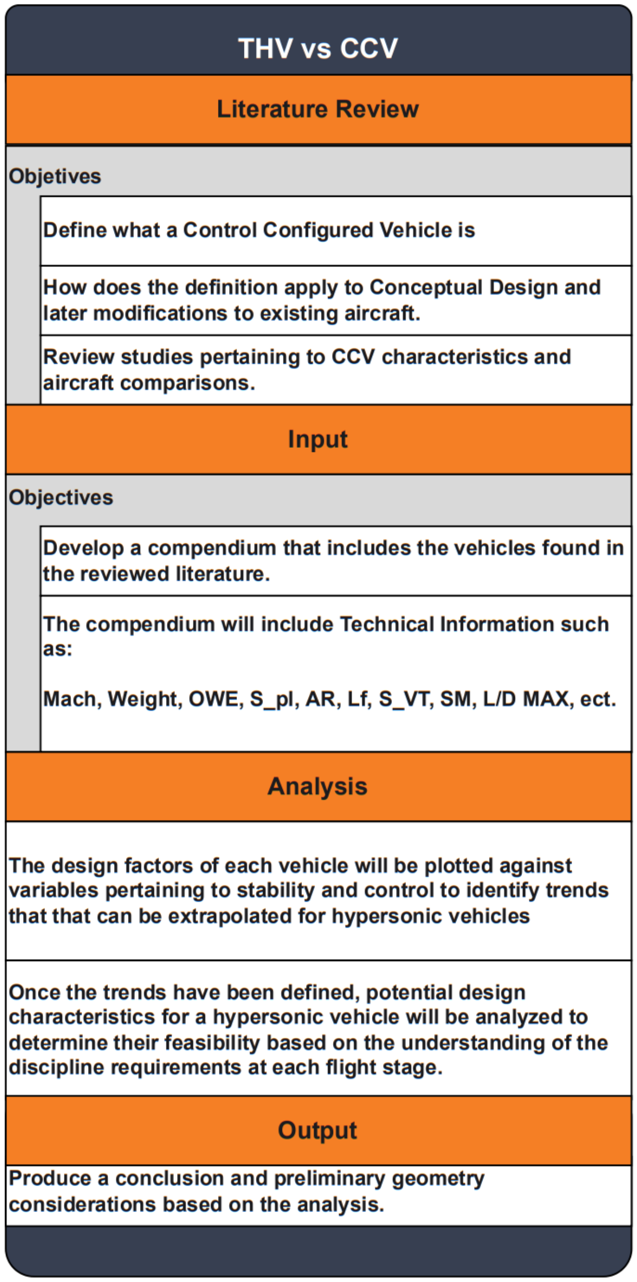

Figure 3.1: NS Diagram of the Methodology

CHAPTER 4

RESULTS AND DISCUSSION

This section presents the trends obtained from the database when compared to parameters relevant to the mission and stability and control. The first subsection presents the trends against Mach number to understand how the vehicle design changes when developed for high-speed missions. This will present an overview of the geometric and performance considerations for high-speed missions, which will provide a baseline of the vehicle that would require more tuning to achieve a CCV status. The second subsection presents the same geometric and performance parameters plotted against the degree of inherent static stability represented via the static margin. This will provide an insight into the changes vehicles experience when their static margin gets reduced to obtain benefits such as weight and drag reductions. Once each trend is discussed, the last subsection will focus on developing a Mach 5 controlled-configured-vehicle by applying the classical methods of using database relationships while also employing the hypersonic regime background to provide an estimate of the feasibility of the configuration.

4.1 Geometric and Performance Trend Behavior against Mach Number

The first parameters to be discussed will be focusing on performance in the ranges of speeds up to Mach 7. As can be seen in Fig. 4.1, the L/D decreases with increasing speed, a behavior that interestingly possesses a trend similar to the decaying behavior of L/D of hypersonic vehicles presented by Kuchemann [27]. This behavior was expected due to the increase of wave drag and skin friction drag as compressibility, and aerothermal effects get more severe at hypersonic speeds. Moving to Fig. 4.2, at lower speeds, vehicles tend to have a more varied range of wing loadings which is supported by the grand variety of missions that take place in this lower speed range. As can be seen for the hypersonic vehicles, they tend to have a low wing loading to a similar range of supersonic fighters. This could be explained by looking at the optimization processes these vehicles undergo, which, due to drag constraints, tend to aim for reduced internal volumes, which decreases the among of weight provided by the payload and the structures required to support a bigger vehicle. Another factor influencing this parameter for the reviewed hypersonic vehicles is the type of mission. Both vehicles were developed to transport a significant amount of payload, either orbital or commercial such as passengers. SAENGER II is an HTO-HL vehicle that constraints its geometry to be efficient not only at its design hypersonic cruise point but also in the subsonic regime, where hypersonic vehicles tend to have poor aerodynamic performance (since they rely on vortex lift, which offers poor lift curve slope) which is often compensated by having a bigger planform area. HEXAFLY-INT is meant to be a boost glide vehicle which also requires a subsonic stage in its mission to deliver the passengers safely. For both scenarios, the vehicles present an increased planform area compared to the same proportion found in the F-4 or the F-16 (which are lighter, hence, having a similar wing loading with a smaller proportion of planform area). The amount of area to generate enough lift for take-off and low speed landing decreases the wing loading of these passenger hypersonic vehicles. This low wing loading can be advantageous to increase maneuverability as well. Moving to Fig. 4.3, it can be seen that the trust-to-weight ratio increases in what appears to be a linear fashion as the speed increases. As can be seen, hypersonic vehicles tend to have the greatest thrust-to-weight ratios, which indicates the high acceleration capabilities of such vehicles, which could be used for maneuverability advantages on hypersonic CCVs.

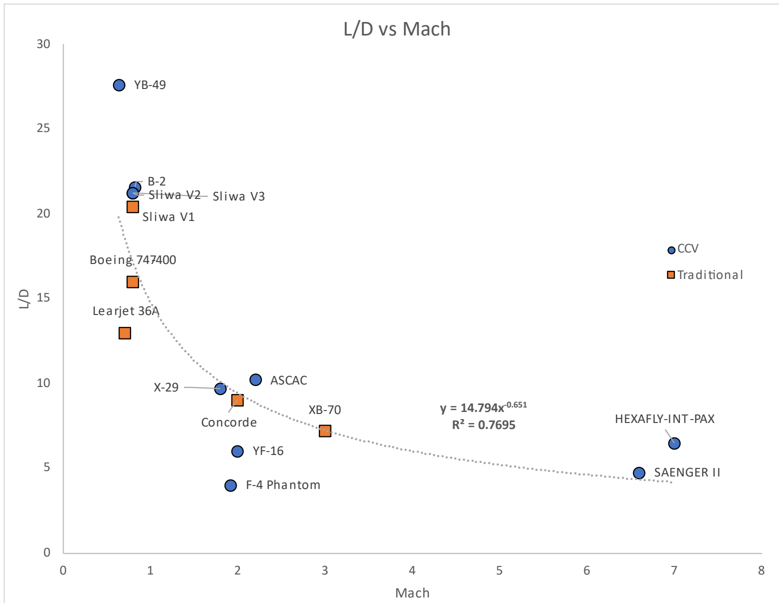

Figure 4.1: Lift-to-Drag Ratio vs. Mach Number

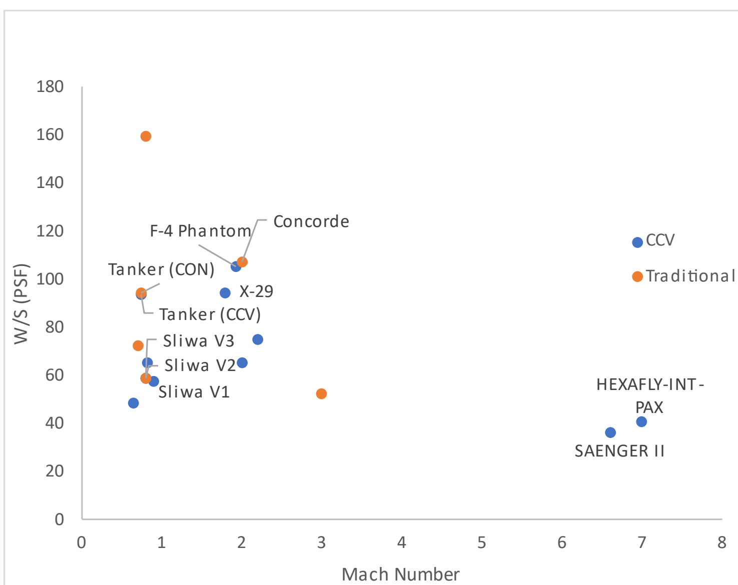

Figure 4.2: Wing Loading vs. Mach Number

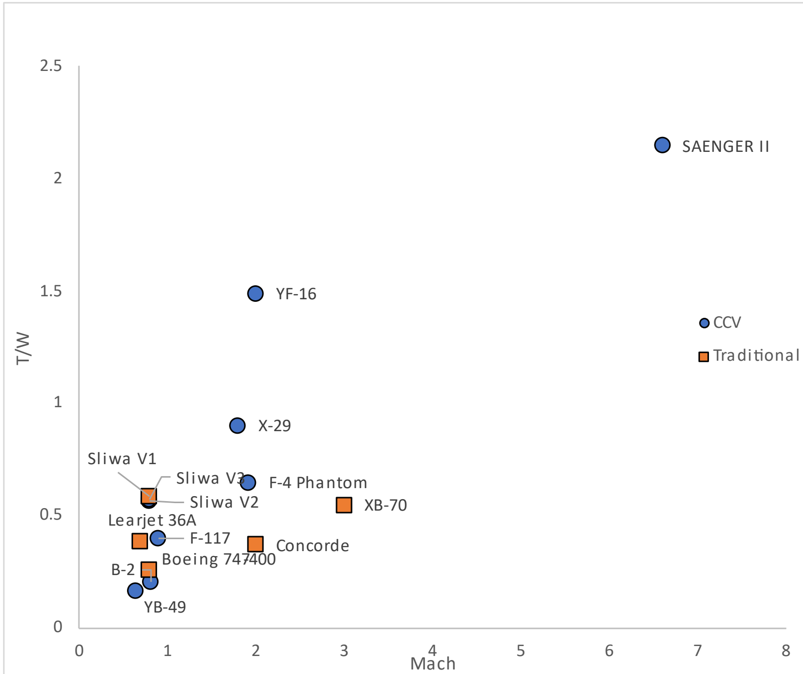

Figure 4.3: Thrust-to-Weight Ratio vs. Mach Number

The second set of parameters pertains to geometrical aspects of the design when compared against the Mach number. Fig. 4.4 shows a significant decrease in the slenderness of the vehicles as the speed is increased. Weiland [24] explains that this occurs due to efforts to reduce wave drag, which arises when vehicles get swept back to increase their subsonic leading edge portion during hypersonic flight. Weiland also states that for slender vehicles, the slenderness ratio should be less than 0.3, which for the SAENGER II and the HEXAFLY-INT is satisfied. This plot also exhibits a more defined decaying tendency that can be used to estimate the slenderness at other speeds between Mach 3 and 6.6. Moving on to Fig. 4.5, the aspect ratio exhibits a decaying behavior with an increase in Mach number, which can be directly attributed to the decrease in the span of these vehicles to reduce wave drag. This might come as a tradeoff between induced drag and skin friction drag for designers since a high aspect ratio is preferable to reduce induced drag and gain performance but to maintain a delta or a compound delta with a high aspect ratio also implies an increase in the wetted area which increases skin friction drag particularly dominant at higher speeds, outweighing the benefit of high aspect ratio. Hypersonic vehicles could potentially eliminate the need for high aspect ratios during the cruise by employing a waverider configuration to allow the generated leading-edge shock to seal the upper and lower surfaces to avoid mixing the pressure distributions.

Regarding the most relevant parameter of this study, the static margin, it can be seen in Fig. 4.6. that a lower speeds vehicles tend to have a more varied range of static stability, which could be attributed to higher aerodynamic efficiency at lower speeds which allows for better control power when using augmented systems to control the vehicle. As the speed increases, the static margin range begins to narrow down to where it appears to converge at RSS, meaning that hypersonic vehicles could be in the range of what could be considered a control configured vehicle due to low degree of inherent static stability. One explanation for this interesting behavior could be due to the dominant aft mass distribution, which can be caused by the placement of the propulsion system these vehicles have, which draws the center of gravity aft, and since the planforms are already swept back, which means the aerodynamic center/neutral point is also shifted back which leaves very small flexibility to achieve a positive static margin. Another explanation for this behavior is that as speed is increased, control surfaces tend to lose control power. If one considers a stable hypersonic vehicle, the magnitude of the restoring moments being generated would be great. In order to maneuver and/or trim the aircraft, large forces would be required, which are very difficult to produce. This reasoning is also supported by a study performed by Scallion [28]. For Fig. 4.7 and Fig.4.8, a progressive reduction in the longitudinal control effector volume coefficient can be seen, which could be attributed to the reduced static margin at high speeds. Regarding the directional control effector volume coefficient of hypersonic vehicles, it does not present much reduction due to the significant decrease in vertical fin effectiveness and loss of directional stability at high speeds. The HEXA-FLY INT outlier is mainly due to a very forward center of gravity location (at 44% of the length), which increases the moment arm and its big dual fins and increases the volume coefficient significantly.

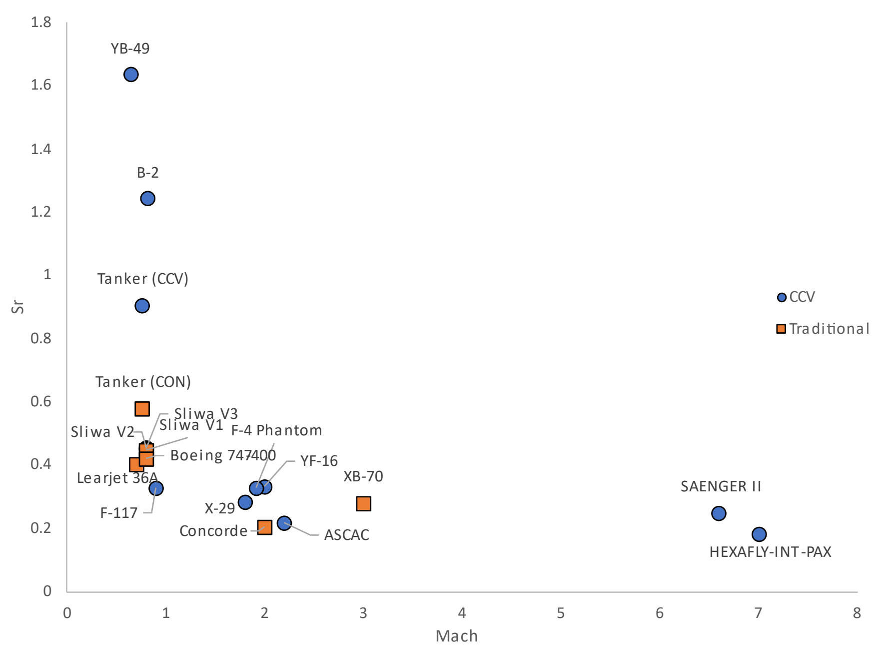

Figure 4.4: Slenderness Ratio vs. Mach Number

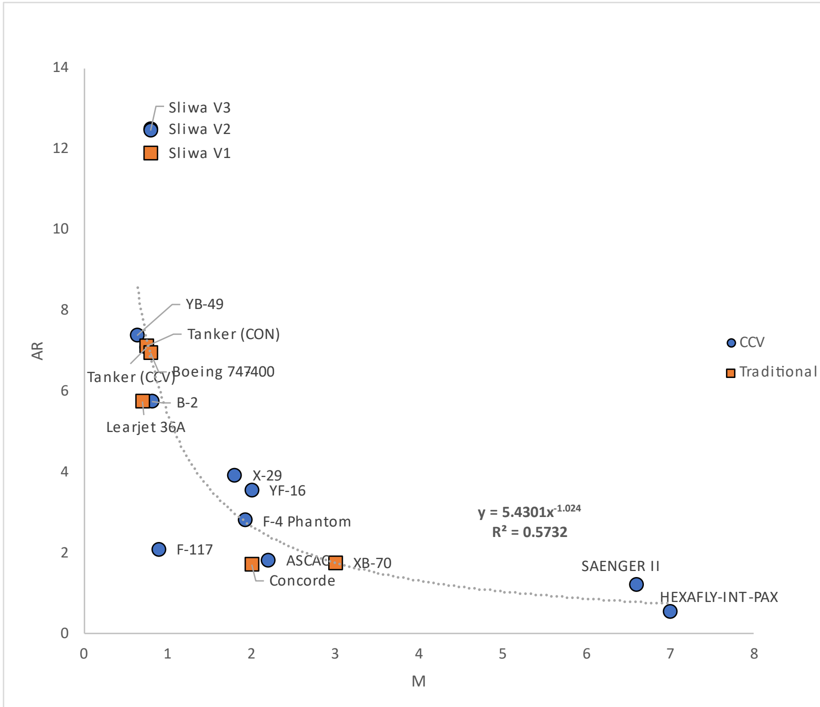

Figure 4.5: Aspect Ratio vs. Mach Number

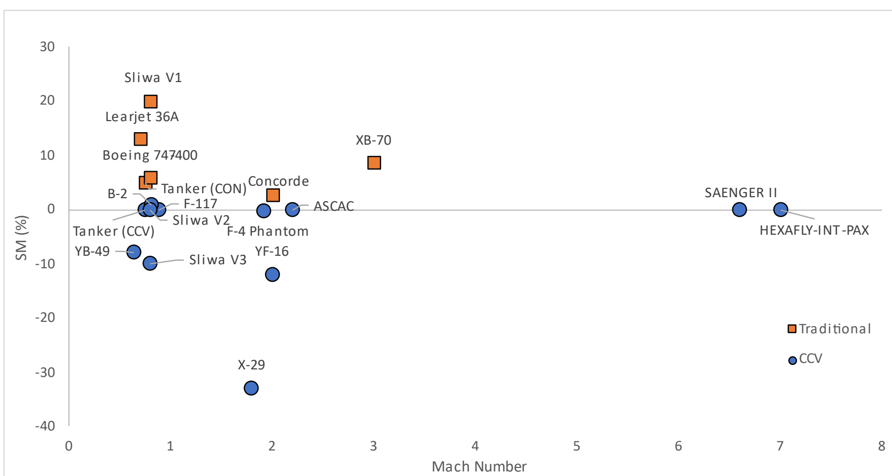

Figure 4.6: Static Margin vs. Mach Number

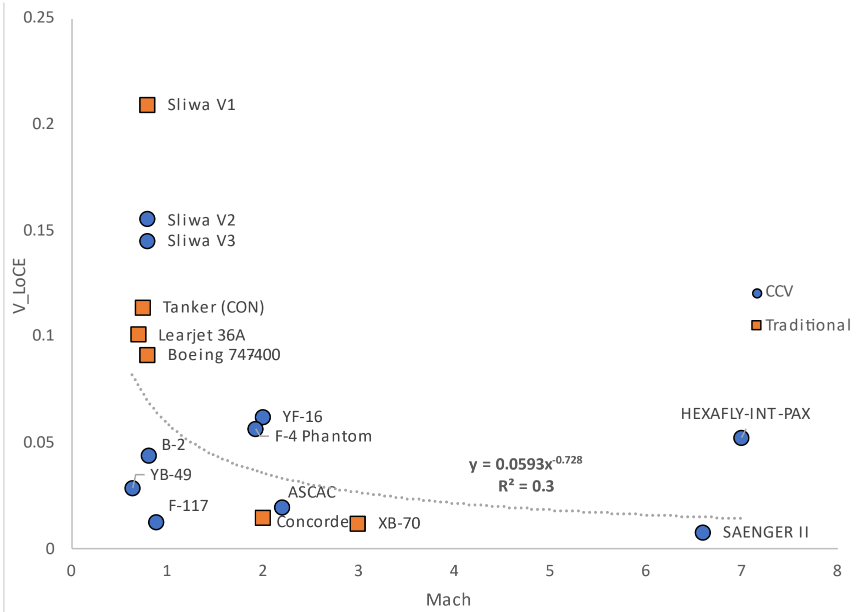

Figure 4.7: Longitudinal Control Effector Volume Coefficient vs. Mach Number

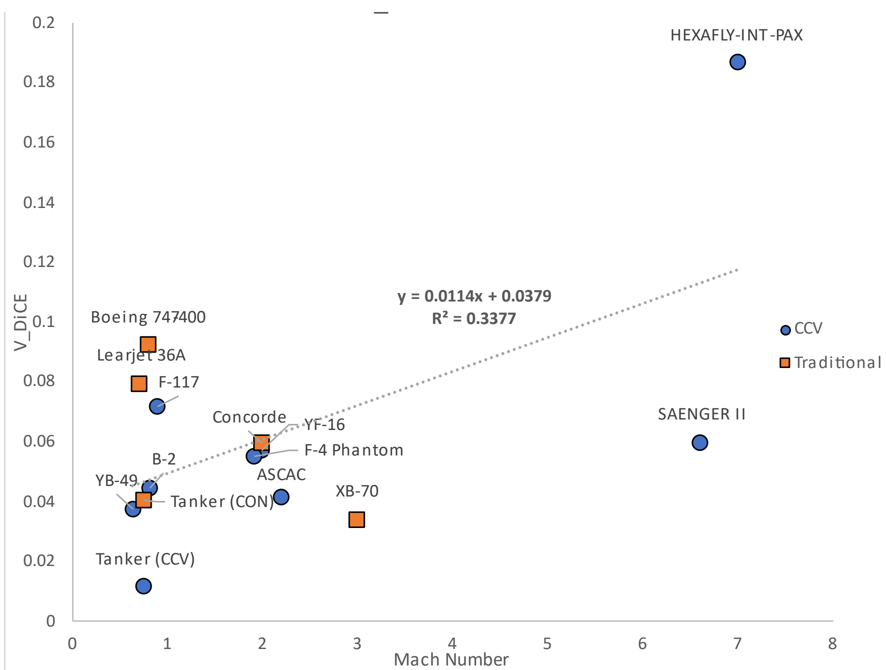

Figure 4.8: Directional Control Effector Volume Coefficient vs. Mach Number

4.2 Geometric and Performance Trend Behavior against Static Margin

Now that the trends with respect to Mach number have been presented, it is equally important for the purposes of this project to identify the trends that occur when one decreases the degree of inherent static stability to RSS and unstable values by decreasing the static margin. This section will play a critical role in identifying CCVs' potential gains and geometry modifications. Overlying this analysis with the characteristics identified in the previous section will provide insight into a Hypersonic CCV.

Starting with the performance aspects, Fig. 4.9. shows that CCVs cover a wider range of L/D ratios than traditional vehicles. Depending on the mission, CCVs can have ratios in the upper 20s for tailless aircraft such as the YB-49 and the B2, whose lack of tail and unstable margin decrease both skin friction and trim drag increasing their L/D significantly. The L/D for hypersonic vehicles, in this case, is lower due to the aerodynamic effects discussed previously but at an RSS condition which indicates that if the vehicles were to be more stable, their L/D could drop below 4 mainly due to an increase in trim drag. Fig. 4.10 shows that CCVs tend to have lower wing loading, which could be attributed to the decrease in weights most vehicles show when they become RSS or unstable. These low wing loadings offer increased maneuverability characteristics for fighters, which tend to be a desired characteristic for CCVs. Finally, Fig. 4.11 shows that CCVs tend to have higher Thrust-to-Weight ratios in part due to CCV weight savings but also because for these vehicles, a significant amount of weight is taken for the propulsion system itself, hence making the overall ratio slightly closer to the T/W of the engine (but of course, lower). Higher thrust-to-weight ratios (at least greater than 1) are desired if thrust vectoring is to be considered for supermaneuvrability characteristics such as the one exhibited by the F-22 Raptor.

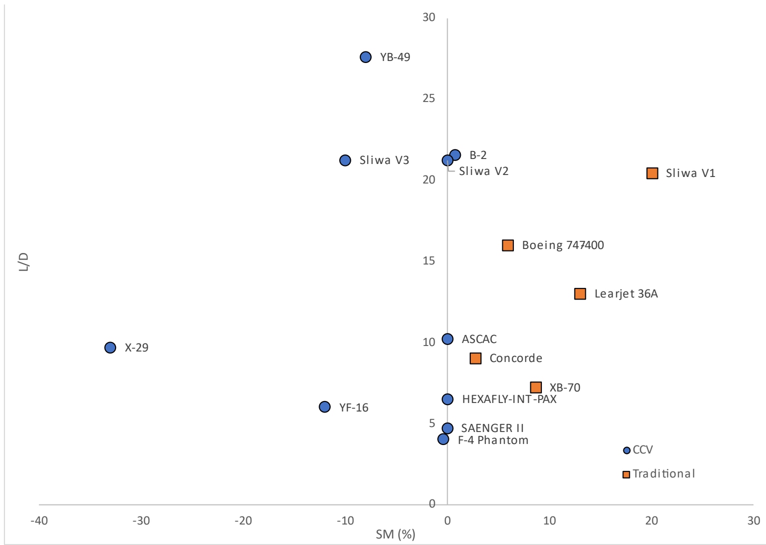

Fig. 4.9: Lift-to-Drag Ratio vs. Static Margin

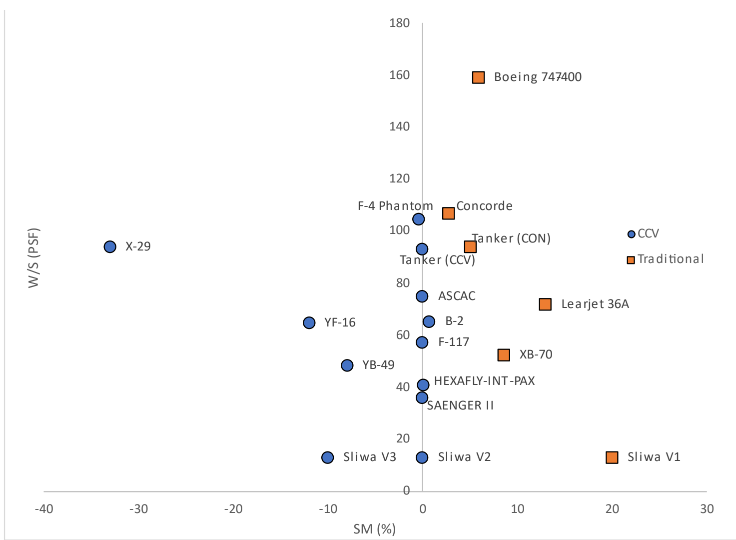

Figure 4.10: Wing Loading vs. Static Margin

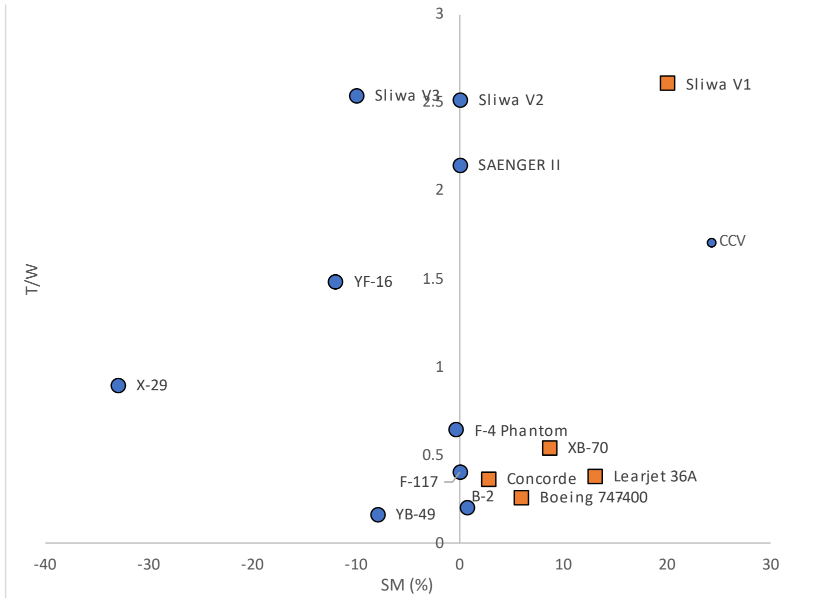

Figure 4.11: Thrust-to-Weight Ratio vs. Static Margin

Regarding geometric parameters, it can be seen that CCV comparative studies show slight increases in slenderness ratio (see the Sliwa [8] and Tanker[9] Vehicles) due to reductions in required length due to the partial or total removal of the horizontal tail. In the case of hypersonic vehicles, these tend to keep a similar proportion to vehicles such as the XB-70 and Concorde, which are lower than other conventional vehicles by having a ratio lower than 0.3 to reduce wave drag stated by Weiland [24]. Regarding Aspect ratio, Fig. 4.12 shows that High speed RSS vehicles tend to have smaller aspect ratios influenced potentially by the degree of sweep their designs have for low drag. Since also these vehicles tend to have a lower slenderness ratio due to the smaller span, the smaller span also translates into decreases in the aspect ratio. Regarding control effector volume coefficients, for the longitudinal case shown in Fig. 4.13, CCVs tend to be more grouped in the lower section of the plot, which could be explained due to the fact that since they are RSS or unstable, they do not encounter as much resistance to attitude changes than if they had a positive static margin such as the traditional vehicles which can be seen in the upper part of the plot mainly to the aft location of their elevators. Suppose one focuses on the configuration differences of the Sliwa and Tanker vehicles. In that case, they exhibit a progressive decrease in volume coefficient as their stability gets reduced by virtue of control effector surface and moment arm reductions. In the case of directional control effector volume coefficient, Fig. 4.14 shows that size reduction is comparably smaller for vehicles with CCVs with high-speed cruises regardless of variations of static margin. This is because the static margin does not significantly influence the directional motion and high-speed vehicles need greater volume coefficients to compensate for control effector efficiency losses.

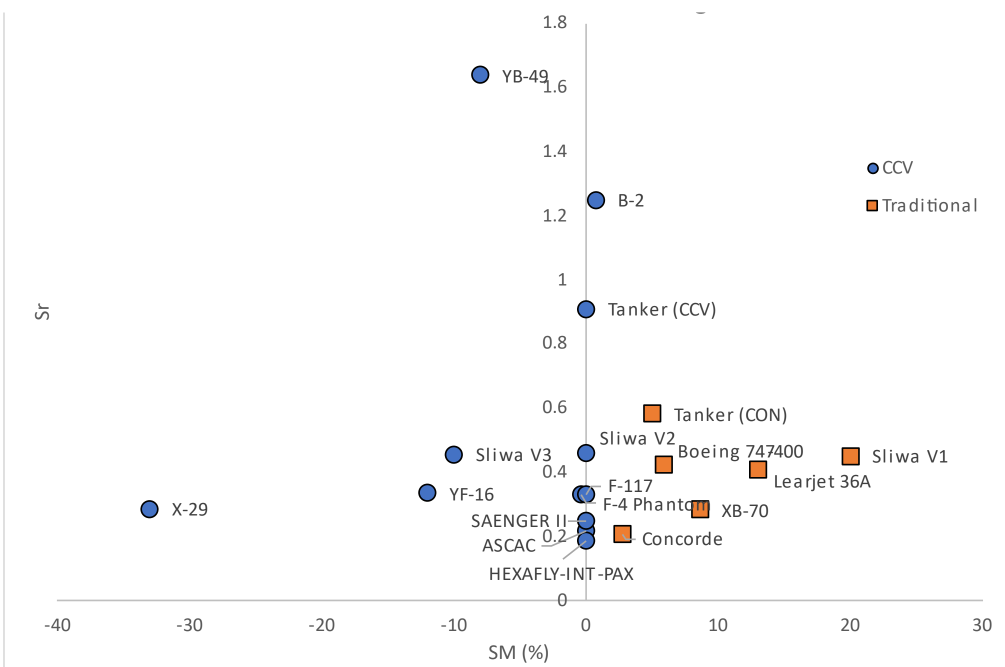

Figure 4.12: Slenderness Ratio vs. Static Margin

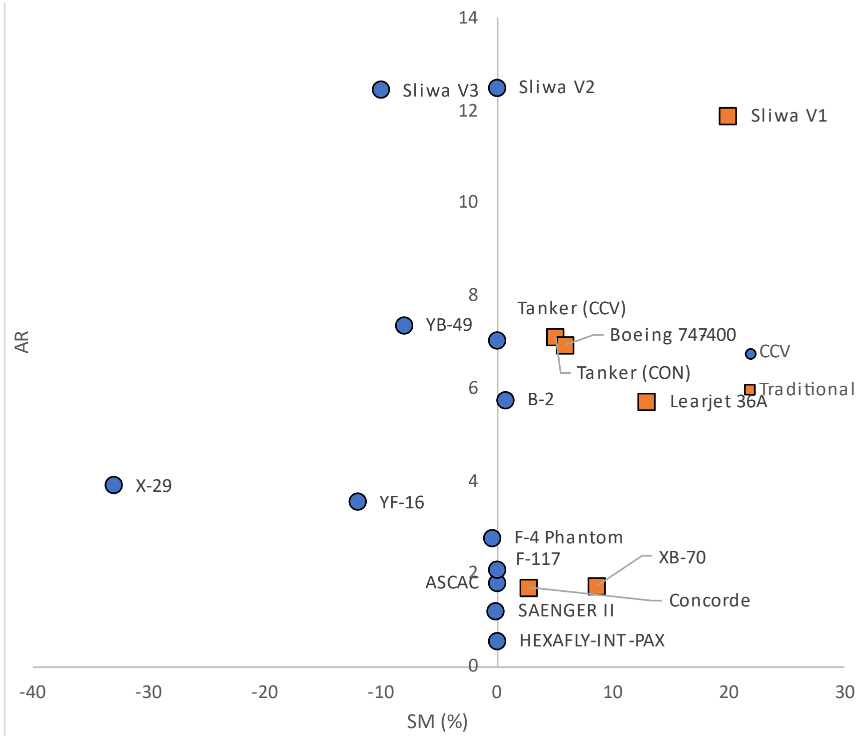

Figure 4.13: Aspect Ratio vs. Static Margin

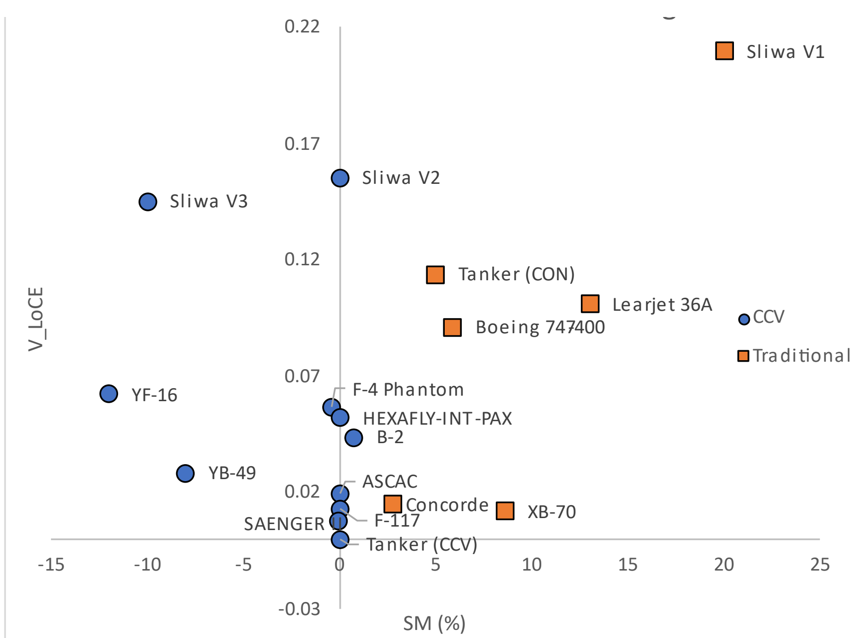

Figure 4.14: Longitudinal Control Effector Volume Coefficient vs. Static Margin

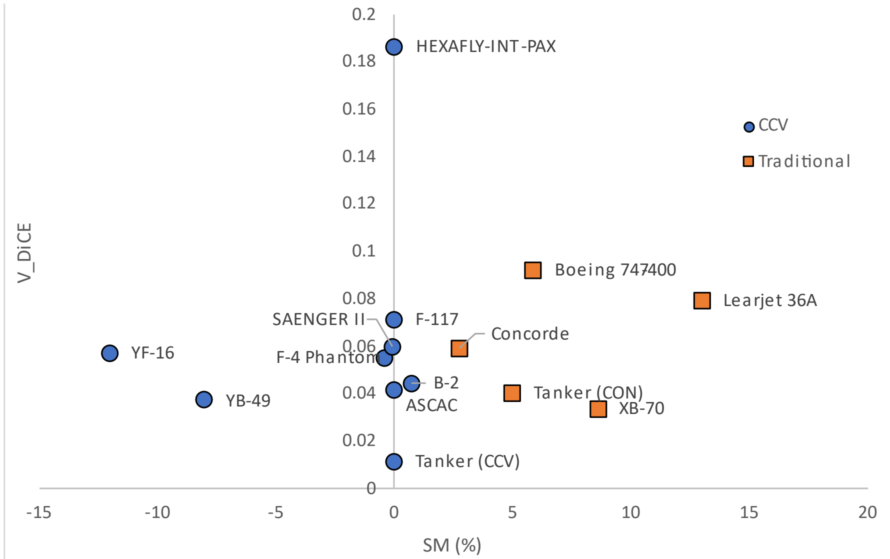

Figure 4.15: Longitudinal Control Effector Volume Coefficient vs. Static Margin

4.3 Determination of Hypersonic CCV Design Point and Evaluation

Now that the major trends and parameter behaviors have been identified and discussed, they are now applied to the design of a controlled-configured-hypersonic vehicle. For this, one needs to define some mission characteristics around which the design process will revolve. For the purposes of this project, the mission requirements will be qualitative, and the design will be assessed numerically based on the trends from the database.

As discussed, if designers have the aerodynamic performance at hypersonic speeds as a main priority of the mission, the most reasonable type of hypersonic vehicle for this task would be a boost glide unmanned vehicle. The reason for this is to take advantage of the waverider configuration as much as possible to generate the greatest hypersonic L/D. As discussed in the previous chapters, waveriders do not offer the greatest volume efficiency for the internal allocation of components, so the lack of a cabin and fuel tanks makes the glider a more viable option. Hence by limiting the trajectory to a glide from the apogee achieved by a rocket stage, the glider can make use of the better waverider performance.

Moving on to wing loading, a glider would need to be highly maneuverable, especially for defense purposes; hence a low wing loading is desired within the boundaries delimited by weights and planform geometry. Due to the lack of complex internal components, the waverider glider could also see weight reductions in its structure, which could decrease the wing loading.

Regarding stability and control, the glider can take advantage of longitudinal unstable static stability, given it has sufficient control power to correct itself as needed. This will significantly reduce the amount of control surface needed, which reduces the size of actuators, decreasing weight, aiding in the desired low wing loading as well., but as discussed by Scallion [28], control effectors that require deflections tend to lose control power significantly so a mixed configuration of controls (such as elevons plus a set of slanted dual fins that act as "ruddervators," as seen by both SAENGER II and HEXAFLY-INT) could be explored. The set of dual fins would benefit from the generation of vortices of the planform if placed correctly due to the reenergizing effect vortices have as they travel aft and hit the surfaces in an SR-71 fashion which could result in improvements in directional stability and DiCE efficiency. To reduce the hinge moments that need to be overcome for proper deflection rates, the inclusion of horns on the elevons (tiperons) such as the ones implemented in the LoFLYTE could be used to produce a counter moment to relieve the load on the actuator, which could translate into further weight savings when using smaller actuators. It is important to note that the degree of instability should be kept conservative since the more complex the control system, the heavier it becomes, and having to use a heavy one would neutralize the efforts to reduce weight in other areas of the configuration, as Hepler et al. concluded [10].

The specific aerothermal characteristics such as materials and leading-edge geometry to reduce heating are beyond the scope of this study, so for the purposes of this analysis, it is assumed that the materials chosen and the geometry are determined in such a way that proves to have a lesser detrimental effect on weights and aerodynamic performance. A summary of the Mission requirements per discipline is presented in Table. 4.1.

Table. 4.1: Summary of Mission Requirements per Discipline

Discipline	Requirements	How can it be achieved
Aerodynamics	High Hypersonic L/D	Employing a Waverider Configuration
SWB	Weight Reduction	Lack of fuel tanks, cabin, propulsion system
Stability and Control	Conservative negative static margin	Control Augmentation System, Slanted Dual Fins, Tiperons
Performance	Maximum glide range	Maximize L/D, reduce trim drag

For the determination of the actual geometry of the glider, determining the L/D for Mach 5.2 should be the first step. Based on Fig. 4.1, by using the curve fit obtained by the decaying trend, the L/D estimated for Mach 5.2 is approximately 5.058, which turns out to be slightly better than the hypersonic configurations surveyed. Using this value, the aspect ratio can be estimated using the curve fit shown in Fig. 4.5, yielding an aspect ratio of 1.004. With this aspect ratio value, Fig. 4.16 can be used to obtain an estimated slenderness value using a curve fit. The slenderness results in a value of 0.221, which is greater than the 0.2 requirement for waveriders presented by Kuchemann [27] in Figure , which falls in the category of waverider, verifying the intent of the configuration. Now that the planform geometry proportions have been established, the LoCE and DiCE volume coefficients will be estimated based on curve fits found on the speed trends shown in Fig. 4.7. and Figure 4.8. and verified with the static margin trends found in Fig. 4.14 and Fig. 4.15. This yields a LoCE volume coefficient of 0.0179, which is comparable to the SAENGER II, and a DiCE volume coefficient of 0.0972, which lies in the range estimated for SANGER II and HEXAFLY-INT.

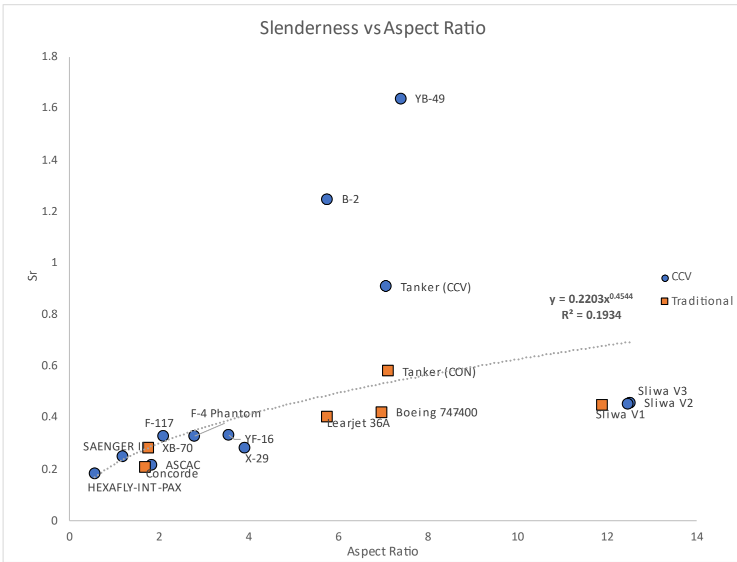

Figure 4.16: Slenderness vs. Aspect Ratio

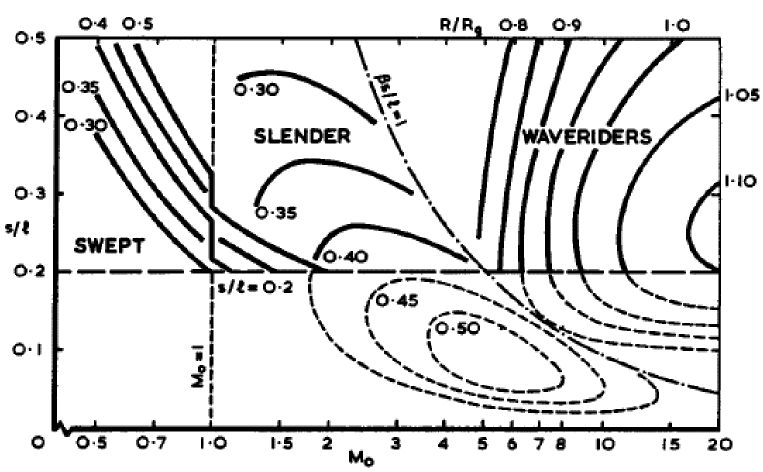

Figure 4.17: Vehicle Type Dictated by Slenderness and Mach Number [27]

Having determined the general geometry characteristics for the Mach 5.2 Hypersonic CCV Glider, the results are summarized in Table. 4.2. Renderings of the model using a unit length as reference are shown in Figure 4.18 through Figure 4.21.

Table. 4.2: Mach 5.2 Hypersonic CCV Glider Characteristics

L/D	SM	AR	S_r	$\bar{V}_{LoCE}$	$\bar{V}_{DiCE}$
5.058	-4%	1.004	0.221	0.0179	0.0972

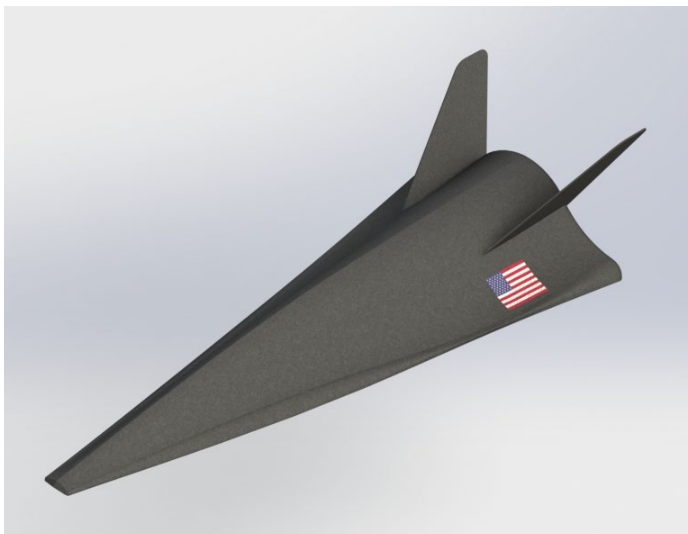

Figure 4.18: Derived CCV Concept Render Isometric View

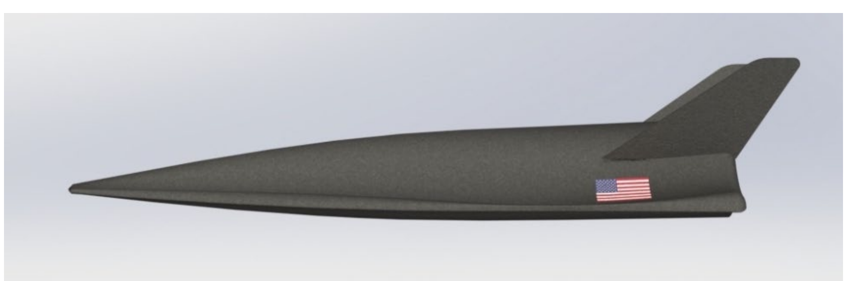

Figure 4.19: Derived CCV Concept Render Side View

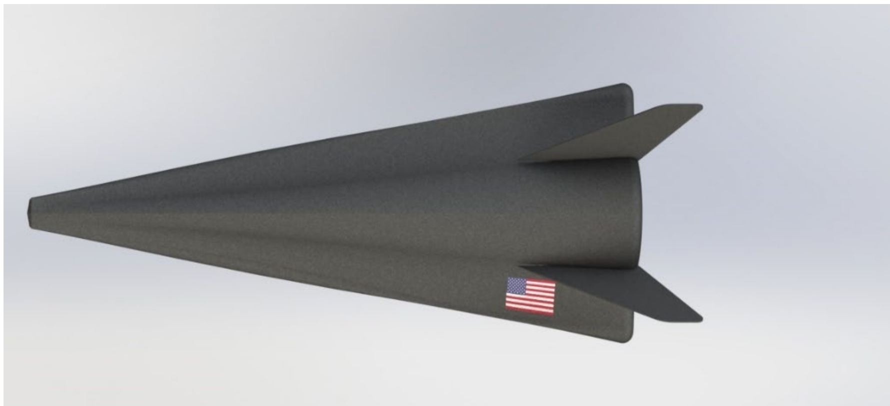

Figure 4.20: Derived CCV Concept Render Top View

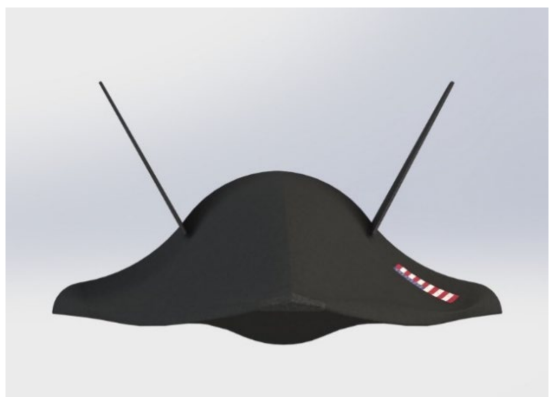

Figure 4.21: Derived CCV Concept Render Front View

CHAPTER 5

CONCLUSION

Stability and control play a fundamental role in the conceptual design of vehicles by producing significant changes in terms of geometry, performance, and weights. As multiple sources have concluded, control-configured-vehicles offer advantages in terms of performance by reducing the wing load of vehicles, increasing thrust to weight ratio, and decreasing the amount of trim drag produced when deflecting a control effector to maneuver and trim traditional inherently stable configurations, which ultimately increases the L/D of the vehicle and hence producing performance improvements.

Geometry changes are more significant in low-speed vehicles due to better aerodynamic efficiency. Most of the significant changes are performed on the horizontal tail either by reducing its area or removing it completely while using a control augmented system to compensate for the impact on handling qualities. Changes to the tail will not be applicable to hypersonic vehicles, so based on the reviewed literature, significant changes can be obtained by changing the internal layout, which impacts internal volume, which changes the cross-section of the vehicle. Such changes can also alter the weight distribution based on component placement and structural weight changes.

Based on the trends, it is interesting to point out that vehicles tend to have a wider range of possible static margins at lower speeds, which allow for a great variety of missions. Still, as speed increases, the range narrows down to Relaxed Static Stability. The literature shows that aerodynamic control power gets significantly reduced at higher speeds regarding control effectiveness. Based on this mixed configuration, such as “tiperons” plus slanted “ruddervators “to increase control power are concepts that can be further explored and evaluated using higher fidelity methods such as wind tunnel testing and computational tools. If aerodynamic control power is not enough to trim the vehicle nor increase its maneuverability, tested control technologies such as thrust vectoring and RCS or cutting-edge technology such as plasma actuation can be implemented in addition to the conventional aerodynamic controls.

The applicability of the control-configured concepts seems to have already been applied to a certain degree on hypersonic vehicles based on the Relaxed stability that both surveyed hypersonic vehicles possess. Based on this, CCV studies could be focused on unstable configurations with missions that occur entirely in the atmosphere, such as boost gliding, and extended missions in the atmosphere, such as commercial transports. Based on the literature reviewed, it can be concluded that the ideal hypersonic CCV needs to minimize its weights and internal volume to obtain maximum aerodynamic performance, which, as of 2022, can only be provided with waverider airframes. Based on this geometry requirement, the ideal CCV will most likely be an unmanned glider with a boost glide mission that could use the first stage to accelerate the vehicle to hypersonic speeds without having to implement a complex propulsion system having a detrimental impact on the waverider’s geometry and weight.

APPENDIX A

LIST OF SYMBOLS

TABLE OF SYMBOLS

AR	=	aspect ratio
b	=	span
c.g.	=	center of gravity
DiCE	=	directional control effector
M	=	cruise Mach number
MAC	=	mean aerodynamic chord
L_f	=	full length of vehicle
LoCE	=	longitudinal control effector
$(L/D)_{MAX}$	=	maximum lift-to-drag ratio
OWE	=	operating weight empty
SM	=	static margin
S_r	=	slenderness ratio
S_{PL}	=	wing planform area
S_{VT}	=	vertical tail surface area
S_{HO}	=	horizontal/LoCE tail surface area
T	=	thrust
TOGW	=	take
T/W	=	thrust-to-weight ratio
W/S	=	wing loading
$\overline{V_{LoCE}}$	=	longitudinal control effector volume coefficient
$\overline{V_{DiCE}}$	=	longitudinal control effector volume coefficient
$\overline{V_{DiCE}}$	=	reference volume coefficient
X_{cg}	=	location of the center of gravity
X_{np}	=	location of the neutral point

APPENDIX B

AIRCRAFT DATABASE

AIRCRAFT	CATEGORY	CRUISE SPE	W (lbs)	OWE (lbs)	T (lb)	S_wing (ft^2)	W/S (psf)	T/W	AR	b (ft)	MAC (ft)	Full Length (ft)	Fuselage Length (ft)	S_V (ft2)	S_ho (ft2)	XCG/C	SM	L/D MAX	Slenderness Rat	L_LoCE (FT)	L_DiCE	V_LoCE REF (f	V_DiCE REF (ft^3)	Vbar_DiCE	Vbar_LoCE
ASCAC	CCV	2.2	750000			10000	75		1.8225	135	65	310	310	676.920738	622.4468467	35	0	10.2	0.217741935	98.7757009	83.157321	3100000	1350000	0.041696974	0.019833104
YF-16	CCV	2	19500		29000	300	65	1.487179487	3.559325	32.67717	9.09	49	49	43.2193201	62.0745977	35	-12	6	0.33344051	14.7762353	13.025294	14700	9803.151	0.057424838	0.062396521
F-4 Phantom	CCV	1.919	55597		35800	530	104.9	0.643919636	2.796698	38.5		58.25	58.25	57.9495205	75.27661143	32.5	-0.4	4	0.330472103	23.3289963	19.464684	30872.5	20405	0.055279054	0.056883239
Tanker (CCV)	CCV	0.75	835,900	250,300		8,940	93.5011186		7.06957	251		138.3	125	571.2	0		0		0.908893709	25.5480296	45.645813	1236402	2247516	0.011600758	
F-117	CCV	0.89	52500	29500	21080	913	57.5216391	0.40152381	2.086149	43.63517		66	66	168.123992	76.84299347	65	0		0.33056947	10.2086331	16.97482	60238.2	39825.81966	0.071658902	0.013022665
B-2	CCV	0.818	336500	158000	69200	5,140	65.4669261	0.20564636	5.755642	172	29.76	69	69	0	693.8318971	47.56	0.739	21.54	1.246376812	22.4347826	56.899811	354660	884080	0.044655352	0.043889832
X-29	CCV	1.8	17800	13800	16000	189	94.279661	0.898876404	3.918114	27.19816	7.22	48	48	32.51	14.32	-14.4	-33	9.68	0.283314167			9062.4	5135.012608		
Sliwa V2	CCV	0.8	118000		66768.273	2001.0109	58.9701935	0.565832822	12.5	158.1538		172.9003	172.9003		580.17421		0	21.2	0.45735559	92.70301		345975.3849	316467.5523		0.155455844
Sliwa V3	CCV	0.8	116000		66245	1975	58.7341772	0.571077586	12.46	156.871		172.9003	172.9003		534.96583		-10	21.2	0.453645731	92.70301		341478.0925	309820.158		0.145230232
YB-49	CCV	0.64	194007	88405	32000	4000	48.50175	0.164942502	7.387403	171.9		52.5	52.5	0	523.1609894		-8	27.6	1.637142857	11.5330426	49.361422	210000	687600	0.037556676	0.028731609
HEXAFLY-INT -PAX	CCV	7	881849.049			21489.11211	41.0370165		0.555615	109.2688	196.85	295.276	295.276	2948.28684	2066.361127	44	0.025	6.5	0.185028249	160.149695	148.88917	6345219.067	2348089.542	0.186946865	0.052153771
SAENGER II	CCV	6.6	559000		1,200,000	15446.21	36.1901075	2.146690519	1.193927	135.8	270.6693	270.6693	270.6693	1853.5452	741.41808	66	-0.05	4.72	0.250859628	46.013781	67.667325	4180814.848	2097595.318	0.059794396	0.00816
Tanker (CON)	Traditional	0.75	1,000,000	334,100		10,640	93.9849624		7.107613	275		236.8	197	1,173	2,310		5		0.580658784	124.228411	101.58087	2519552	2926000	0.040722612	0.113896291
Concorde	Traditional	2	412000	173500	152000	3,856	106.846473	0.368932039	1.7	83.9895	90.74	202.29659	202.29659	365	344.44	59	2.73	9	0.207590004	33.8701299	52.922078	780055.651	323863.512	0.059644133	0.014955635
Sliwa V1	Traditional	0.8	118000		69160	2016	58.531746	0.586101695	11.9	154.8883		172.9003	172.9003		788.99387		20	20.4	0.447912314	92.70301		348567.0048	312254.9073		0.209836576
XB-70	Traditional	3	331000		180000	6297.8	52.5580361	0.543806647	1.751	105	78.54	185.75	185.75	467.92	270.52	23.9	8.6	7.2	0.282637954	51.9852941	48.073529	1169816.35	661269	0.03401727	0.012021598
Learjet 36A	Traditional	0.7	18300	10119	7000	253.3	72.2463482	0.382513661	5.74	39.5		48.66666667	48.66666667	41.8432441	58.62883829	32	13	13	0.405821918	21.2431271	19.003436	12327.26667	10005.35	0.079474024	0.10103293
Boeing 747-400	Traditional	0.8	877000		226607	5500	159.454545	0.258388826	6.96099	195.6667	27.3	231.8333333	231.8333333	1008.91952	1108.315908	13	5.886	16	0.421998562	105.176755	98.543987	1275083.333	1076166.667	0.092386203	0.091420747

APPENDIX C

DIC CALCULATIONS

Span		
ft	172	
pix	529	
Scale	0.325142	
l_LoCE	69	22.43478
l_DiCE	175	56.89981

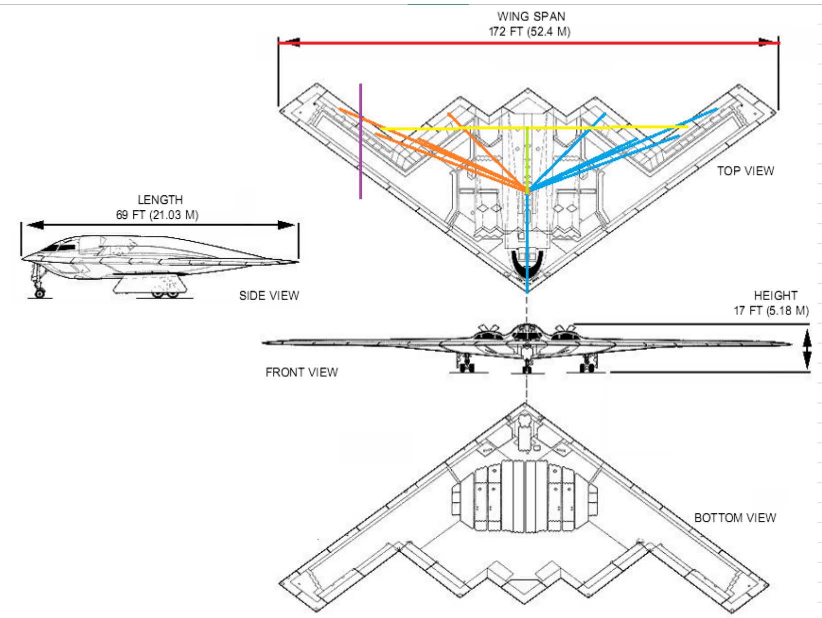

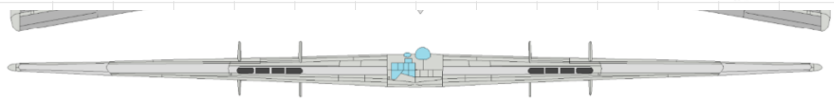

TRAD		
length		
ft	236.8	
pix	711	
Scale	0.333052	ft/pix
	PIX	ft
l_LoCE	373	124.2284
l_DiCE	305	101.5809

CCV		
length		
ft	138.3	
pix	406	
Scale	0.34064	
	pix	ft
	75	25.54803
	134	45.64581

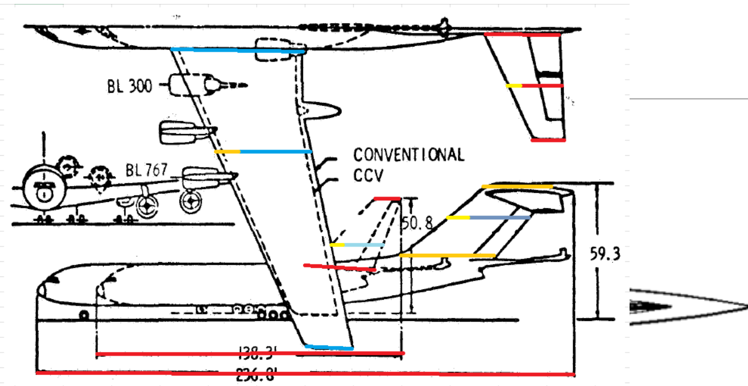

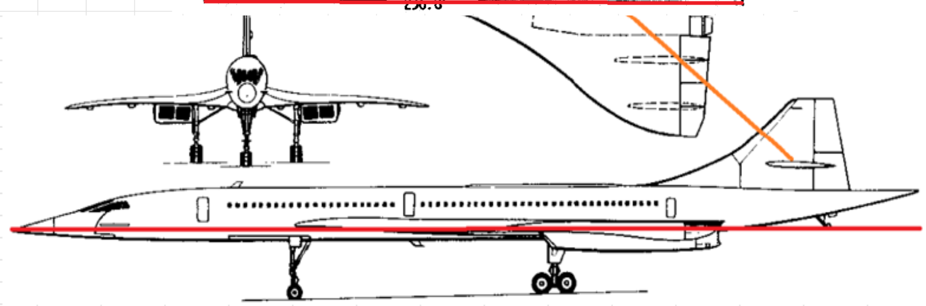

Span		
ft	32.67	
pix	765	
Scale	0.042706	ft/pix
	pix	ft
MAC	213	9.096353
	pix	ft
A1	188	8.028706
A2	66	2.818588
A3	134	5.722588
1 HT S	31.0373	ft2
Total HT	62.0746	ft2
	pix	ft
B1	364	15.54494
B2	207	8.840118
B3	43	1.836353
C1	43	1.836353
C2	98	4.185176
C3	162	6.918353
LowerVT	22.38979	
UpperVT	20.82953	
TotalVT	43.21932	ft2
l_LoCE	346	14.77624
l_DiCE	305	13.02529

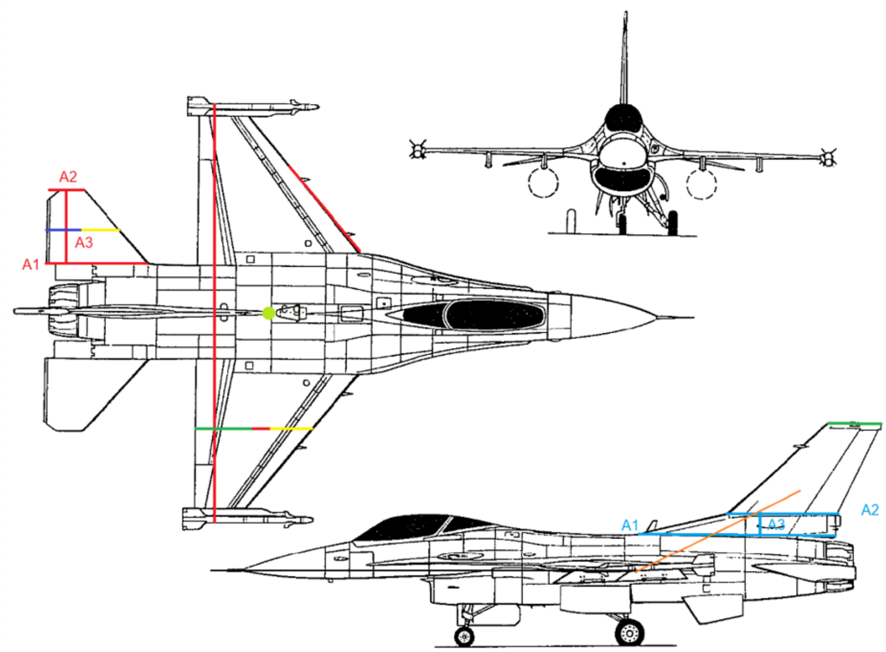

Span		
ft	39.5	
pix	582	
Scale	0.067869	
A1	73	4.954467
A2	42	2.850515
A3	110.679	7.511719
1 HT S	29.31442	ft2
Total HT	58.62884	ft2
B1	133	9.026632
B2	75	5.090206
B3	84	5.701031
C1	58	3.936426
C2	12	0.814433
Trapezoid	40.24027	
Triangle V	1.602978	
Total VT	41.84324	ft2
MAC	109.21	7.412019
l_LoCE	313	21.24313
l_DiCE	280	19.00344

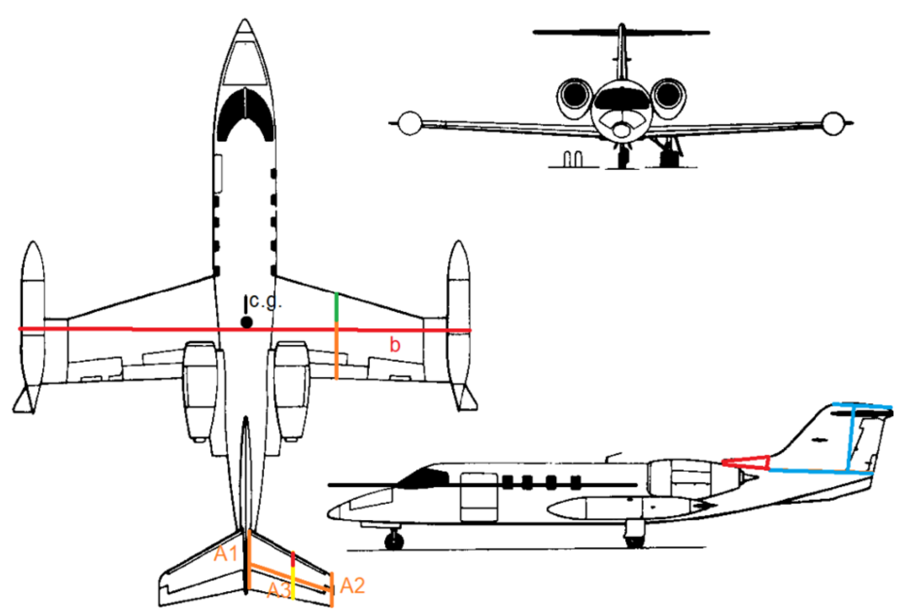

Span		
ft	135.5	
pix	321	
Scale	0.422118	
	pix	ft
A1	105	44.32243
A2	26	10.97508
A3	58	24.48287
VT	676.9207	ft^2
B1	72.1734	30.46572
B2	11	4.643302
B3	42	17.72897
1 HT S	311.2234	
Total LoCE	622.4468	ft^2
l_LoCE	234	98.7757
l_DiCE	197	83.15732

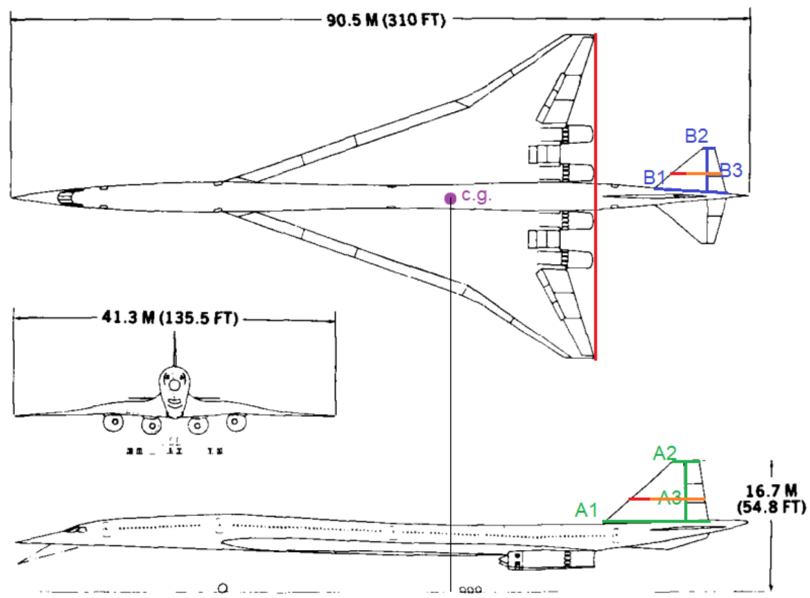

(a) Configuration details.

LoCE S tot	2066.361	ft^2
B1	160	66.72904
B2	54	22.52105
B3	63	26.27456
C1	54.4	22.68787
C2	21	8.758186
C3	46	19.1846
1 VT	1172.503	ft^2
1 Rudder	301.64	ft^2
1 VT total	1474.143	ft^2
Total DiCE	2948.287	ft^2
	pix	ft
D1	87	36.28392
D2	262	109.2688
Spl	21489.11	ft^2
l_LoCE	384	160.1497
l_DiCE	357	148.8892

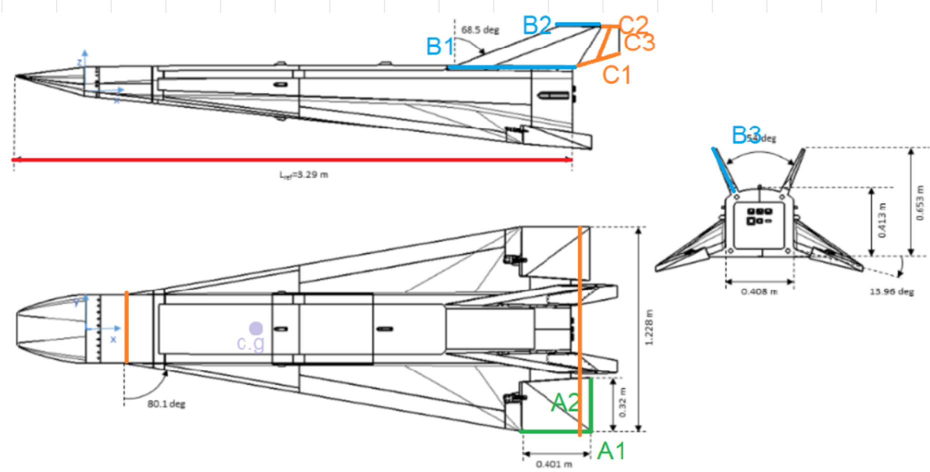

Span			
ft	105		
pix	1020		
scale	0.102941	ft/pix	159.6738
A1	94	9.676471	
A2	202	20.79412	
l_LoCE	505	51.98529	
l_DiCE	467	48.07353	

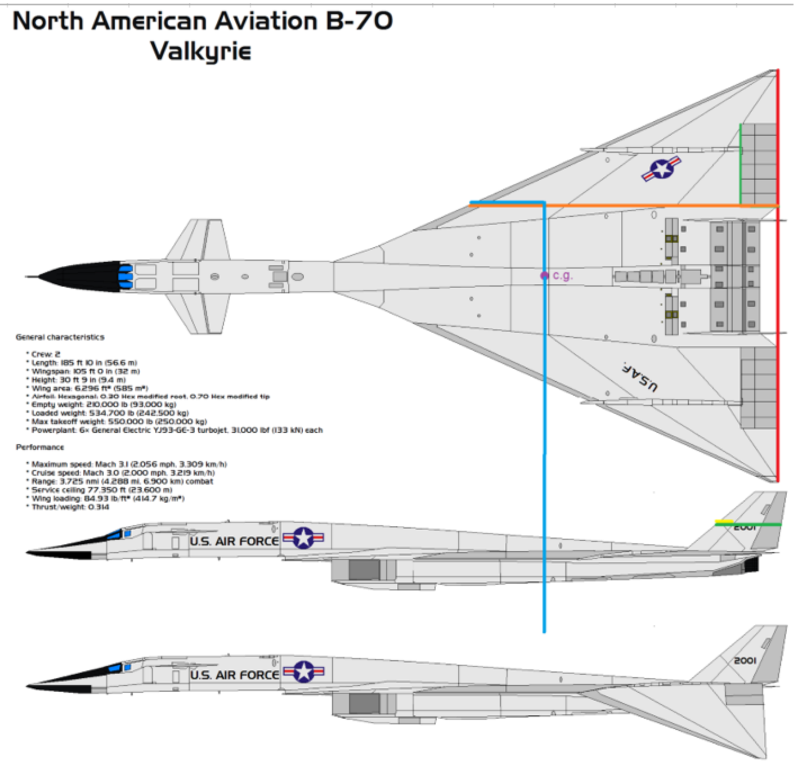

	span	
ft	172	
pix	659	
scale	0.261002	ft/pix
	pix	ft
A1	22.2	5.794234
A2	134.52	35.10992
Outer Elevon S	203.4351	ft
Total	406.8702	
B1	19.2	5.011229
B2	109.7	28.63187
Inner Elevon	143.4808	
Ttal	286.9617	
Total Elevon S	693.8319	ft^2

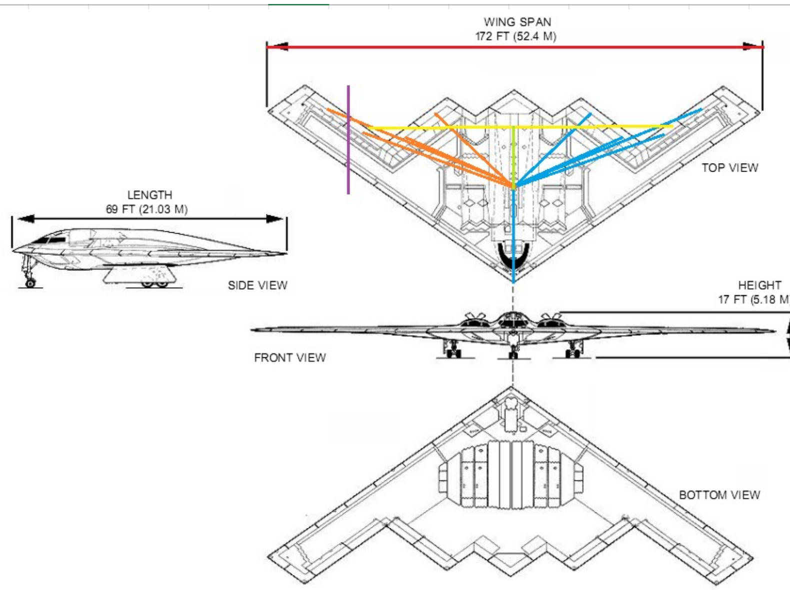

Span	
ft	38.5
pix	269
Scale	0.143123

	pix	ft
A1	53.6	7.671375
A2	16	2.289963
A3	52.8	7.556877
1 HT S	37.63831	ft2
TOTAL HT	75.27661	ft2

	pix	ft
B1	110	15.74349
B2	28	4.007435
B3	41	5.86803
VT	57.94952	ft2

	pix	ft
l_LoCE	163	23.329
l_DiCE	136	19.46468

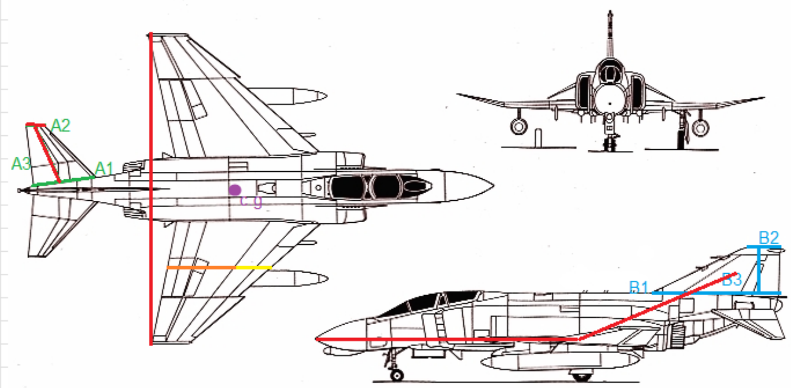

	Length	
ft	66	
pix	556	
scale	0.118705	ft/pix

	PIX	FT
A1	16.278	1.932281
A2	115.624	13.72515
A3	30.8868	3.666419
Elevon	38.4215	ft2
Total Elev	76.84299	ft2
B1	44	5.223022
B2	86	10.20863
B3	91.78	10.89475
VT	84.062	ft^2
Total Vt	168.124	ft^2
l_LoCE	86	10.20863
l_DiCE	143	16.97482

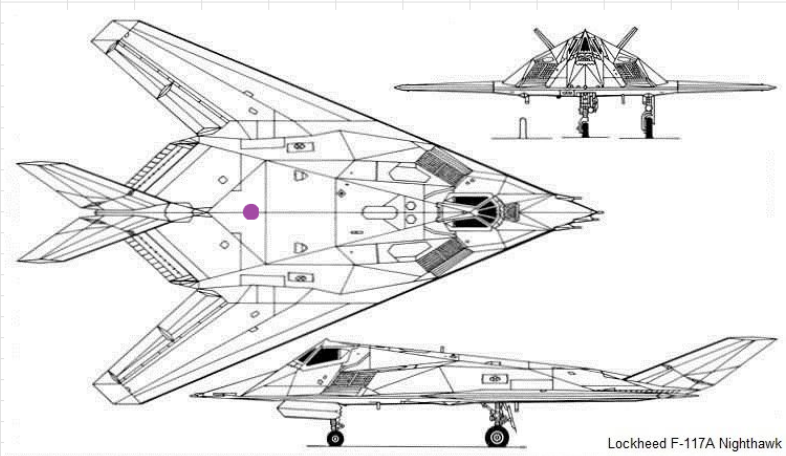

Span		
ft	195.6667	
pix	826	
Scale	0.236885	ft/pix

	pix	ft
A1	103.16	24.43701
A2	34	8.054076
A3	144	34.11138

1 Elevator	554.158	ft^2
Total	1108.316	ft^2

B1	161	38.13842
B2	51	12.08111
B3	169.62	40.18036

VT	1008.92	ft^2

	pix	ft
l_LoCE	444	105.1768
l_DiCE	416	98.54399

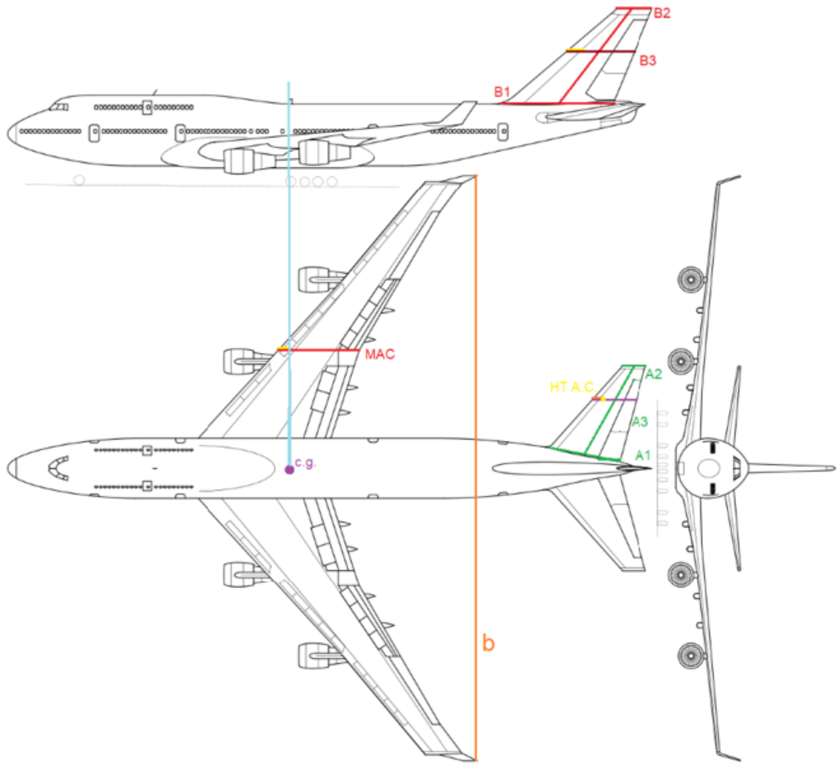

Span		
ft	156.6	
pix	299	
Scale	0.523746	

	pix	ft
l_LoCE	177	92.70301
l_DiCE	166	86.94181

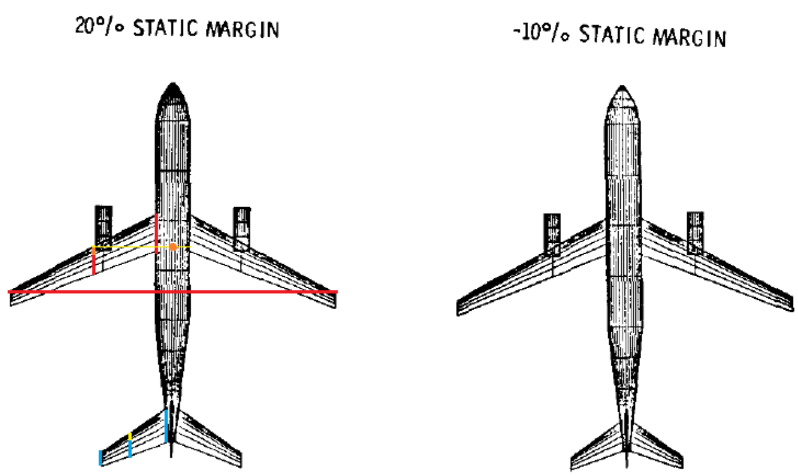

REFERENCES

[1] Weiland, C. *Aerodynamic Data of Space Vehicles*. Springer, 2014.

[2] Anderson, J. *Fundamentals of Aerodynamics*. McGraw Hill Education, New York, New York, 2017.

[3] Al-lami, H., Aslam, A., and Quigley, T. The Evolution of Flight Control Systems. University of West England-Bristol, Feb 28, 2015.

[4] Culick, F., and Jex, H. Aerodynamics, Stability and Control of the 1903 Wright Flyer. American Institute of Aeronautics and Astronautics, Inc., Nov 20, 1984.

[5] Yechout, T. *Introduction to Aircraft Flight Mechanics, Performance, Static Stability, Dynamic Stability, and Classical Feedback Control*. American Institute of Aeronautics and Astronautics, Inc., Reston, Virginia, The United States of America, 2003.

[6] Nygren, K. Breguet's Formulas for Aircraft Range and Endurance: An Application of Integral Calculus.

[7] Roskam, J. *Part VII: Determination of Stability, Control and Performance Characteristics: FAR and Military Requirements*. DAR Corporation, 2002.

[8] Sliwa, S. Impact of Longitudinal Flying Qualities Upon the Design of a Transport with Active Controls. Nasa.

[9] Walker, S. Design of a Control Configured Tanker Aircraft. Wright-Patterson Air Force Base.

[10] Hepler, A., Zeck, H., Walker, W., and Shafer, D. Applicability of the Control Configured Design Approach to Advanced Earth Orbital Transportation Systems. NASA, 1978.

[11] Wolowics, C., and Strutz, L. Preliminary Flight Evaluation of The Stability and Control Derivatives and Dynamic Characteristics of the Unaugmented Xb-70- 1 Airplane Including Comparisons with Predictions. NASA, May, 1968.

[12] Nicolai, L., and Carichner, G. *Fundamentals of Aircraft and Airship Design*. American Institute of Aeronautics and Astronautics.

[13] StockphotosArt. XB-70 Valkyrie. .

[14] Chudoba, B. *Stability and Control of Conventional and Unconventional Aerospace Vehicle Configurations - A Generic Approach from Subsonic to Hypersonic Speeds*. Springer Aerospace Technology, Arlington, TX, 2019.

[15] Anderson, M. R., and Mason, W. H. An MDO Approach to Control-Configured-Vehicle Design. American Institute of Aeronautics and Astronautics, Inc., 1996.

[16] Ashkenas, I., and Klyde, D. Tailless Aircraft Performance Improvements with Relaxed Static Stability. NASA, Mar, 1989.

[17] Krachmalnick, J., and Lafavor, S. Air Superiority with Controlled Configured Fighters. American Institute of Aeronautics and Astronautics, Inc., 1971.

[18] Swortzel, F., and Finley Barfield, A. The CCV Fighter Program - Demonstrating New Control Methods for Tactical Aircraft. American Institute of Aeronautics and Astronautics, Inc., 1976.

[19] Dickeson, J., and Rodriguez, A. Elevator Sizing, Placement, and Control-Relevant Tradeoffs for Hypersonic Vehicles. American Institute of Aeronautics and Astronautics, Inc.

[20] Rainey, R. Static Stability and Control of Hypersonic Gliders. NACA, Jul 07, 1958.

[21] Wimpenny, J. C. Stability and Control in Aircraft Design. May, 1954.

[22] Cameron, D., and Princen, N. Control Allocation Challenges and Requirements for the Blended Wing Body.

[23] Zahringer, C. *Untersuchung Der Separationsdynamik Eines Zweistu¯gen Hyperschall-Flugsystems Unter Besonderer BerÄucksichtigung Der Seitenbewegung*. Technischen Universitat Munchen, Munich, Germany, 2004.

[24] Weiland, C., and Hirschel, E. H. *Selected Aerothermodynamic Design Problems of Hypersonic Flight Vehicles*. Springer, 2009.

[25] de Castro, H. V. *The Longitudinal Static Stability of Tailless Aircraft*. Cranfield University, 2001.

[26] Morani, G., Nebula, F., and Di Donato, M. Trajectory and Flight Mechanics Analysis of the HEXAFLY-INT Experimental Flight Vehicle. HiSST: International Conference on High-Speed Vehicle Science Technology, Nov, 2018.

[27] Kuchemann, D. *The Aerodynamic Design of Aircraft*. AIAA, Reston, Virginia, The United States of America, 2012.

[28] Scallion, W. Aerodynamic Characteristics and Control Effectiveness of the HL-20 Lifting Body Configuration at Mach 10 in Air. NASA, Sep, 1999.

[29] Encyclopedia Britannica. F-16 Aircraft. Britannica, Apr 03, 2019.

[30] Boeing. Boeing: Historical Snapshot: F-4 Phantom II Fighter. *Boeing*. https://www.boeing.com/history/products/f-4-phantom-ii.page. Accessed Apr. 25, 2022.

[31] F-117A. F-117A: Production Specifications. *f-117A*. http://www.f-117a.com/Specs.html.

[32] Piccirillo, A. C., and Aronstein, D. C. *Have Blue and the F-117A: Evolution of the Stealth Fighter*. Reston, Va, 1997.

[33] Sherman, R. F-117A Nighthawk - Military Aircraft. *Military Analysis Network*. https://man.fas.org/dod-101/sys/ac/f-117.htm.

[34] Northrop Group. B-2 Technical Details. *Northrop Grumman*. https://www.northropgrumman.com/what-we-do/air/b-2-stealth-bomber/b-2-technical-details. Accessed Apr. 25, 2022.

[35] Grumman X-29. *Military Wiki*. https://military-history.fandom.com/wiki/Grumman_X-29. Accessed Apr. 25, 2022.

[36] Saltzman, E. J., and Hicks, J. W. “In-Flight Lift-Drag Characteristics for a Forward-Swept-Wing Aircraft (and Comparisons With Contemporary Aircraft).” *Nasa Technical Paper*, No. 3414, 1994, p. 60.

[37] Military Factory. Northrop YB-49. *Military Factory*. https://www.militaryfactory.com/aircraft/detail.php?aircraft_id=977.

[38] Herutage Concorde. Heritage Concorde. *Airframe Dimensions*. https://www.heritageconcorde.com/airframe-dimensions.

[39] Airliners. LearJet. *Airliners.net*. https://www.airliners.net/aircraft-data/learjet-313536/265.

[40] Learjet 75 Specifications, Cabin Dimensions, Performance. *GlobalAir.com*. https://www.globalair.com/aircraft-for-sale/Specifications?specid=1420. Accessed Mar. 2, 2022.

[41] Min, K., Plumley, R., and Brooks, A. Boeing 747. , 2007.

[42] Modern Airlaines. Boeing 747 Specs. *Modern Airliners*. https://modernairliners.com/boeing-747-jumbo/boeing-747-specs/.

[43] Romli, F., and Kamaruddin, M. “Preliminary Study of Emissions Regulation Effects on Future Commercial Aircraft Designs.” *International Journal of Environmental Science and Development*, Vol. 4, 2013, pp. 187–190. https://doi.org/10.7763/IJESD.2013.V4.332.

[44] Buritica Yate, J. *On Stability and Control and Geometry Development in the Conceptual Design Stage of Generic Hypersonic Vehicles*. The University of Texas at Arlington, 2021.

BIOGRAPHICAL INFORMATION

Juan Camilo Buriticá Yate is a Colombian student pursuing an Honors Bachelor of Science in Aerospace and Mechanical Engineering at the University of Texas at Arlington. His interests in the aerospace industry focus on vehicle design, flight mechanics, Computational Fluid Dynamics, and dynamic simulations of aircraft trajectories. Besides college, he has been working as an engineering collaborator for the ATLAS Experiment at CERN under the supervision of Dr. Haleh Hadavand for the Low Voltage Power Supply Research group at the University of Texas at Arlington.